Deciphering a marine bone degrading microbiome reveals a complex community effort

Erik Borchert[a,#], Antonio García-Moyano[b], Sergio Sanchez-Carrillo[c], Thomas G. Dahlgren[b], Beate M. Slaby[a], Gro Elin Kjæreng Bjerga[b], Manuel Ferrer[c], Sören Franzenburg[d] and Ute Hentschel[a,e]

[a]GEOMAR Helmholtz Centre for Ocean Research, RD3 Research Unit Marine Symbioses, Kiel, Germany

[b]NORCE Norwegian Research Centre, Bergen, Norway

[c]CSIC, Institute of Catalysis, Madrid, Spain

[d]IKMB, Institute of Clinical Molecular Biology, University of Kiel, Kiel, Germany

[e]Christian-Albrechts University of Kiel, Kiel, Germany

Running Head: Marine bone degrading microbiome

[#]Address correspondence to Erik Borchert, eborchert@geomar.de

Abstract word count: 250

Text word count: 4926 (excluding Abstract, Importance, Materials and Methods)

Abstract

The marine bone biome is a complex assemblage of macro- and microorganisms, however the enzymatic repertoire to access bone-derived nutrients remains unknown. The resilient structure of collagen in bones, its main organic component and its interwoven character with inorganic hydroxyapatite makes it however difficult to be exploited as an organic resource. To study the microbial assemblages harnessing organic bone components as nutrients, we conducted field experiments with the placement of bovine and turkey bones at 69 m depth in a Norwegian fjord (Byfjorden, Bergen). Metagenomic sequence analysis was used to assess the functional potential of microbial assemblages from bone surface and the bone eating worm *Osedax mucofloris* that is a frequent colonizer of whale falls and known to degrade bone. The bone microbiome displayed a surprising taxonomic diversity and novelty revealed by the examination of 59 high quality metagenome assembled genomes from at least 23 different bacterial families. Over 700 enzymes from twelve relevant enzymatic families pertaining to collagenases, peptidases, glycosidases putatively involved in bone degradation were identified. This study allowed us to decipher the bone degrading microbiome that initiates demineralization of inorganic bone components by a closed sulfur biogeochemical cycle between sulfur-oxidizing and sulfur-reducing bacteria leading to a drop in pH and subsequent processing of organic components. An unusually large collagen utilization gene cluster was retrieved from one genome belonging to the γ-proteobacterial genus *Colwellia*. The gene cluster displayed a significant degree of novelty in comparison to clusters present in closely related *Colwellia* strains, none yet described in detail.

Importance

In this metagenomic study we decipher the interactions, pathways and enzymes that are necessary to access and utilize the organic bone matrix in the marine microbial space. Bones are an underexploited, yet potentially profitable feedstock for biotechnological advances and value chains, due to the sheer amounts of residues produced by the modern meat and poultry processing industry. We herein demonstrate the interplay between core community members from specialist to generalist and present a toolbox of enzymes with the potential to cover an array of reactions relating to the bone matrix components. We identify and describe a novel gene cluster for collagen utilization. The bone microbiome is a perfect example of an extraordinarily complex microbial assemblage, that is only able to function and survive due to the interplay between the different community members across taxonomic borders.

Introduction

The marine environment is a treasure trove for novel microbial assemblages, organic catalysts (enzymes) and biochemical reactions biocatalysts (1-3). The oceans cover approximately 70% of the Earth surface with an estimated volume of about 2×10^{18} m^3 and due to its incredible environmental variability (e.g. temperature, pressure, salinity, light availability), it has sparked the evolution of an unprecedented range of different microbes and hence enzymatic activities (4-7). Genome sequencing of individual microbial isolates of complex communities has allowed us to get a glimpse of their diversity and their potential functions. The underrepresentation of cultivable microbes has advanced functional and sequence-driven metagenomic analyses, and enabled us to decipher complex interactions in entire microbial consortia (8-13).

The deep-sea was for a long time seen as an almost lifeless environment, as no one could imagine life to be possible under conditions vastly different and more extreme than those in shallower ocean waters. Nowadays we know that even the deep-sea is steaming with life; hydrothermal vents, sponge grounds and coral gardens are superb examples of unique and complex habitats (14-16). Nonetheless, the deep-sea is a harsh environment with limited nutrient sources. In this respect sudden events like a whale fall create a locally defined, but huge nutrition source for deep-sea life, that can last for many years or even decades (17). These whale carcasses are usually stripped of their soft tissue rapidly by larger scavengers, but the energy-rich bones remain as a slow nutrient source. More than 15 years ago *Osedax* was described, a genus of bone-eating annelid worms (18), and has since then been investigated for its diversity, ecology and how it accesses the organic compounds of whale bones (18-21). These worms bore cavities into bones and are known to harbor endosymbionts in their root tissue typically affiliated to Oceanospirillales (18, 22-25). In the study area in the northern North Atlantic *Osedax mucofloris*

was described in 2005 and has been shown to consistently colonize bone material on the sea floor below a depth of 30 m (26-28). The species can thus be regarded as a member of the bone biome and an important facilitator in this degradation process.

Bone is a recalcitrant and heterogeneous composite material made of a mineral phase, an organic phase and water. Hydroxyapatite crystals in the mineral phase contribute to the structural strength in bones. The organic phase includes proteins, such as collagen and structural glycoproteins (e.g. proteins decorated with mannose, galactose, glucosamine, galactosamine, N-acetylglucosamine, N-acetylgalactosamine, rhamnose, sialic acid and fucose), lipids and cholesterol composed of various triglycerides (29-31). Up to 90% of the protein content in mature bone is made of type I collagen, a triple helical molecule rich in glycine, hydroxyproline and proline that acquires organization into fibrils with a high degree of hydrogen bonds, hydrophobic interactions and covalent cross-linking, which together confer high structural stability to collagen fibrils (32). It is thus hypothesized that degradation of the recalcitrant bone matrix will require a synergistic multi-enzyme system that likely requires a microbial community effort. This will likely include essential enzymes in the breakdown of the organic matrix, namely collagenases that break the peptide bonds in collagen and other proteases/peptidases that attack the glycoproteins. Furthermore, neuraminidases (sialidases), α-mannosidases, α-/β-galactosidases, α-fucosidase, α-rhamnosidase and α/β-N-acetylhexosaminidase (glucose and galactose-like), all glycoside hydrolase enzymes (COG0383, COG1472, COG3250, COG3669, COG4409, Pfam16499, Pfam16499), are likely involved in cleavage of glycosidic linkages. Finally, in the digestion of the cholesterol-containing marrow, cholesterol oxidases (COG2303) are probably involved.

To date only a few studies have been published that focus on microbial communities to understand the necessary complex interactions in bone degradation, mainly relying on 16S rRNA gene sequencing data (33, 34) and one metagenomic study of a whale fall (35). We here provide a first comprehensive overview and identify putative key functions involved in bone degradation of the marine bone microbiome retrieved from deployed bone material, including microbial communities from the gutless worm *Osedax mucofloris* and free living microbial assemblages developing on the bone surface.

Results

Recovery of artificially deployed bone for bone microbiome metagenomic analysis

To collect relevant bacterial communities, turkey and bovine bones were deployed at 69 m depths in Byfjorden, a fjord outside Bergen, Norway. After several months of incubation, underwater images taken by a remotely operated vehicle (ROV) showed microbial colonization of the bone surfaces (supplementary figure S1A). *Osedax mucofloris* worms were observed, especially on the joints, and in some cases forming small colonies of several individuals inside a single cavity under the external bone tissue. Although not object of this study, a larger diversity of invertebrate fauna including *Ophryotrocha*, *Vigtorniella* and *Capitella* worms were also observed. Dense microbial mats developed asymmetrically with preference for the joint adjacent sections (epiphysis), which also appeared in aquaria settings (supplementary figure S1B).

Two different sets of samples were collected and subjected to metagenome sequencing. The two sets of metagenomes are an *Osedax*-associated bone microbiome (OB), and a bone surface associated biofilm (BB), each consisting of four individual metagenomes (Table 1). Eight individually sequenced metagenomes generated a raw output of approximately 211 mio reads (per direction) yielding a combined assembly of 1.5 Gbp. According to Small Subunit (SSU) rRNA gene abundance calculations, a large fraction (>75%) of the *Osedax*-associated SSU rRNA gene reads accounts for *Osedax* (18S), while the BB metagenome contains less than 5% of eukaryotic SSU rRNA gene affiliated reads. The microbial communities were dominated by four different bacterial classes, these being Campylobacteria (35% in OB, 20% in BB), Desulfobacteria (5,8% in OB, 12,8% in BB), γ-proteobacteria (26,9% in OB, 1,9% in BB) and Bacteroidia (14,3% in OB, 5,5% in BB) although in different proportions (Figure S2B). The OB

metagenome is less diverse than the BB metagenome, with the diversity estimate Chao1 ranging from 286 Operational Taxonomic Units (OTUs) to 566 OTUs respectively (Figure S2A) based on all obtained SSU rRNA gene reads. The bacterial fraction of the OB metagenome consists to approximately 27% of Oceanospirillales affiliated reads, which likely represent *Osedax* endosymbionts (22).

High quality metagenome assembled genomes (MAGs) from the marine bone microbiome display taxonomic diversity and novelty

59 high quality MAGs (>90% completion and <10% redundancy) were extracted from the combined metagenomes (see supplementary Table S1 for MAG sequence statistics). The MAGs span 11 phyla, 14 classes, 19 orders and at least 23 families. About 63% of the MAGs (37/59) possess a taxonomic novelty determined by their relative evolutionary divergence (RED) according to Parks *et al.* (2018) (36) to their closest common ancestor (Table 2). One MAG could be only identified up to phylum level, seven to class level, seven to order level, 18 up to family level and four up to genus level (Figure 1). The taxonomy of most MAGs was fully resolved based on 120 marker genes. The three best represented phyla are Proteobacteria (22 MAGs), Campylobacterota (14 MAGs) and Bacteroidota (8 MAGs), which is consistent with the relative abundances of the metagenomic sequence reads and the 16S RNA gene profiling (Figure S2). However, the percental distribution of the most abundant classes differs considerably between the two metagenome sets. The OB-MAGs were dominated by the classes γ-proteobacteria (27%), Campylobacteria (27%) and α-proteobacteria (20%), while the BB-MAGs were mainly affiliated with γ-proteobacteria (30%), Campylobacteria (23%) and Bacteroidia (16%).

Primary metabolism of the marine bone microbiome

All MAGs were investigated using Multigenomic Entropy Based Score pipeline (MEBS) (37) for their ability to utilize different energy sources (sulfur and nitrogen) via the abundance of selected marker genes for these pathways (Figure 2). MAGs affiliated to the order Campylobacterales (BB9, BB14, BB41 – Sulfurovaceae; BB10, BB26 – Thiovulaceae; OB7, BB28, BB30 – Arcobactereaceae; OB11, BB15 - *Sulfurospirillum* and OB8, OB5, BB11 - *Sulfurimonas*), some unclassified γ-proteobacteria (OB6, BB34, BB36 and BB4) and the γ-proteobacteria affiliated to Beggiatoaceae (BB2, BB3, BB16, BB20 and BB31) are all potentially capable of thiotrophy via utilization of reduced sulfur compounds as electron donors (flavocytochrome c sulfide dehydrogenase (*fcc*B) and adenosine-5'-phospho-sulfate reductase (*apr*AB)) and partial predicted Sox sulfur/thiosulfate oxidation pathway. Additionally, the Campylobacterales MAGs also contain marker genes for the oxidation of sulfite to sulfate via the Sor pathway. MAGs identified as Desulfuromusa (BB21, BB25), Desulfobacteria (BB40 and OB14), Desulfobulbia (BB13) and Desulfovibrionia (OB3) presented the marker genes for dissimilatory sulfite reductase system (*dsr*KMJOP) (also found in the Beggiatoaceae and unclassified γ-proteobacteria MAGs), but they lack Sox and Sor pathway genes. In all γ-proteobacteria (except BB32) and Desulfobacterota (BB13, BB40, OB3 and OB14) genes for dissimilatory sulfite reductase (*dsr*ABC) are present. Müller *et al.* (2015) described that γ-proteobacterial *dsr*AB-type genes are commonly involved in oxidative reactions, whereas *dsr*AB in Desulfobacterota are reductive type *dsr*AB (38). All MAGs contain at least partial pathways for dissimilatory tetrathionate reduction (*ttr*ABC), thiosulfate disproportionation (*phs*ABC and rhodanase) and contain also genes for sulfoacetaldehyde degradation (*isf*D, xsc and *saf*D), nitrate reduction

(assimilatory and dissimilatory), methylamine degradation, sulfolactate degradation, and ammonia assimilation (ammonia assimilation I and superpathway ammonia assimilation).

With respect to microbial bone degradation, the features of gelatin hydrolysis and H_2S production (desulfurylation) were additionally of interest and were investigated using Traitar (39), which provides genome-informed phenotype predictions. 22 MAGs showed capacity of gelatin hydrolysis (19 MAGs in the bone surface community (BB) and three in the *Osedax* associated communities (OB)) and 10 MAGs for H_2S production (six MAGs in BB and three in OB). Traitar's prediction for gelatin hydrolysis is based on the presence of 70 and the absence of 51 other Pfam families. With gelatin being a primarily bone collagen derived compound, we consider gelatin hydrolysis a key trait for the microbial community studied herein. All eight Bacteroidia affiliated MAGs (BB17, B22, BB23, BB24, BB29, BB35, BB42 and OB13) possess the gelatin hydrolysis trait, seven γ-proteobacteria MAGs (BB2, BB3, BB5, BB20 BB32, BB44 and OB12), one tentative Planctomycetota MAG (BB1), one Spirochaetia MAG (BB7), two Krumholzibacteria MAGs (BB18 and BB39), one Thiovulaceae (BB26), one Geopsychrobacteraceae (BB27) and one Fermentibacteria MAG (BB12) (Figure 3). The prediction of the H_2S production trait in Traitar is based on the presence of 43 Pfam families and absence of 22 Pfam families. This trait was identified in 10 MAGs, two of which were Marinifilaceae (OB13 and BB29), two Krumholzibacteria (BB18 and BB39), two *Sulfurospirillum* (OB11 and BB15), one Spirochaetaceae (BB7), two Desulfobacteraceae (OB14 and BB40), and one *Pseudodesulfovibrio* (OB3).

Accessing the recalcitrant bone material by acid-based solubilization

To identify mechanisms key to utilize the resilient bone as a nutrient source, the MAGs were screened for marker genes for enzymatic functions beneficial for bone degradation. In this respect, enzymes catalyzing reactions leading to an acidification of the local environment could be important to increase the solubilization of hydroxyapatite and thereby making the bone's organic matrix more accessible to microbial colonization and enzymatic attack. The obtained bacterial genomes were therefore screened for lactate dehydrogenase (*ldh*), carbonic anhydrase and P-type ATPase. Altogether the MAGs contained 35 annotated lactate dehydrogenases, 191 P-type proton ATPases (H^+-ATPase) and 94 carbonic anhydrases (supplementary table S2). Three lactate dehydrogenases per genome were found in the α-proteobacterial MAGs OB15, OB9 and BB33. Five MAGs (BB6, BB20, BB38, BB42, OB14) contained two lactate dehydrogenases, whereas 16 MAGs contained one lactate dehydrogenase (BB1, BB3, BB5, BB9, BB17, BB18, BB22, BB26, BB29, BB35, BB37, BB40, OB1, OB3, OB8, OB14). The identified lactate dehydrogenases were investigated for the presence of signal peptides to be secreted to the extracellular matrix, but none contained such a signal and therefore do most likely not play a prominent role in acidification. Plasma membrane H^+-ATPases are found in elevated levels (>10) solely in unclassified γ-proteobacteria (BB4, BB34 and BB36) and Beggiatoales affiliated MAGs (BB3, BB16 and BB20), all from the surface attached microbial communities. Only five MAGs are devoid of P-Type ATPases, being BB12 (Fermentibacteriaceae), BB27 (Geopsychrobacteriaceae), OB13 (*Labilibaculum*) BB18 and BB39 (both Krumholzibacteria). Carbonic anhydrases were identified in 51 of 59 MAGs. Nineteen out of 94 carbonic anhydrases contained a signal peptide for extracellular export (16 MAGs). 15 were predicted to contain a Sec signal peptide (SPI) and four to encode lipoprotein (SPII) signal peptides. Four out of five Beggiatoales MAGs were predicted to contain carbonic anhydrases with a SPI signal peptide

(BB2, BB3 and BB20) or a SPII signal peptide (BB16). The remaining three SPII signal peptides were found in carbonic anhydrases from Campylobacterales (BB8, BB10 and BB11), interestingly BB8 contains at least three carbonic anhydrases, one with a SPI, one with a SPII and one without signal peptide. Three SPI signal peptides were found in carbonic anhydrases from unclassified γ-proteobacteria (BB4, BB34 and BB36) mentioned previously alongside Beggiatoales with elevated P-type ATPase levels. The remaining SPI including carbonic anhydrases were found in five Campylobacterales MAGs (BB14, BB26 (three carbonic anhydrases and two containing SPI signal peptides), BB30, BB41 and OB7) and one Desulfobulbaceae MAG (BB13). 18 out of 19 carbonic anhydrases belong to the α-carbonic anhydrase family and one to the β-family, no γ-family carbonic anhydrases were found, based on phylogenetic relationship to known carbonic anhydrases of each family, reference sequences described in Capasso *et al.*, 2015 have been used (40) (Supplementary figure S3).

The anticipated thiotrophy has the potential to contribute massively to the acidification of the environment via the oxidation of reduced sulfur compounds leading to production of sulfuric acid (41). This requires a close interaction between sulfur-reducing bacteria (SRB) producing hydrogen sulfide and sulfur-oxidizing bacteria (SOB) utilizing the hydrogen sulfide, while releasing protons (Figure 3). The Traitar analysis identified 10 MAGs potentially able to produce hydrogen sulfide, including known SRB like Desulfobacteraceae, Pseudodesulfovibrio, and others like *Sulfurospirillum* (42-44). The bone microbiome is especially enriched in known SOB, like the large filamentous bacteria Beggiatoales (5 MAGs) (45) and Campylobacterales (10 MAGs) (46, 47). Furthermore, one MAG identified as Desulfobulbaceae was found in the bone associated metagenomes. These cable bacteria are known to be able to perform sulfur oxidation and sulfur reduction (48, 49).

Enzymatic profiling for enzymes involved in bone degradation

Based on the structure and composition of mature vertebrate bone tissue, we hypothesized that 12 different COGs and peptidase/collagenase families were relevant for the enzymatic attack of the bone organic matrix. This "bone-degradome" comprised the peptidase families S1 (COG0265), S8/S53 (and Pfam00082), U32 (COG0826) and M9 collagenase (including Pfam01752), mannosidases (COG0383), sialidases (COG4409), glucuronidases (COG3250), glucosaminidases (COG1472), galactosaminidases (COG0673), α-galactosidases (Pfam16499), cholesterol oxidases (COG2303) and fucosidases (COG3669). We constructed HMM profiles that were used to screen the abundance of each enzyme family in all MAGs (Figure 4). In total 722 enzymes belonging to the 12 investigated enzyme families were identified in the 59 MAGs. Most enzyme families were widespread (except COG0383, COG3669, COG4409, Pfam16499 and M9 collagenases). M9 collagenases and α-galactosidases (Pfam16499) were only found in three MAGs. The M9 collagenases where solely found in Enterobacterales (BB5, BB44 and OB12). Pfam16499 was only identified in Bacteroidales (BB22, BB24 and OB13). The most abundant group of enzymes were the S1 peptidases (141 hits), followed by galactosaminidases (COG0673) (116 hits) and U32 peptidases (99 hits) (Figure 4), constituting 20%, 16% and 14% of all identified bone degrading enzymes, respectively. In general, Bacteroidales (BB17, BB22, BB24, BB29, BB42 and OB13) displayed the most diverse set of enzyme families related to bone degradation, as they contained genomic evidence of all enzymes besides M9 collagenases. MAGs belonging to the orders Desulfuromonadia, Desulfobulbia, Desulfobacteria, Desulfovibrio, Campylobacteria (all of them driving the sulfur biogeochemical cycle), as well as some undefined α-proteobacteria and γ-proteobacteria appear to have no or few mannosidases

(COG0383), glucuronidases (COG3250), fucosidases (COG3669), sialidases (COG4409) and α-galactosidases (Pfam16499).

Colwellia, the potential degrader of collagen

We investigated the genomic context of each M9 collagenase for potential links to metabolic pathways, such as proline utilization (Supplementary figure S4). *Colwellia* MAG BB5 possessed an approximately 21 kbp-long gene cluster presumably devoted to collagen utilization, which is unique in the dataset and in the public databases. The functional cluster spans at least 15 different genes (Figure 5A), featuring a secreted Zn-dependent M9 collagenase, a secreted peptidyl-prolyl cis-trans isomerase (cyclophilin-type PPIase), a secreted unknown protein and an unknown Zn/Fe chelating domain-containing protein. Additionally, one putative transporter (MFS family), a TonB-dependent receptor and several genes involved in the catabolism of proline and hydroxyproline e.g. prolyl-aminopeptidase YpdF, intracellular peptidyl-prolyl cis-trans isomerase (rotamase), pyrroline reductase, hydroxyproline dipeptidase, 4-hydroxyproline epimerase and others. Moreover, genes involved in transcription regulation such as PutR and the stringent starvation protein A and B were identified.

To explore the conservation of this gene cluster, we retrieved fourteen representative *Colwellia* genomes of marine origin from the NCBI repository (Supplementary table S3). To minimize methodological bias, the nucleotide sequences of these genomes were likewise annotated with RAST (Rapid Annotation using Subsystem Technology) and screened for M9 collagenase using the previously established HMM profile. Up to 22 annotated M9 collagenases were identified in the seven genomes. In the genomes of *Colwellia piezophila* ATCC BAA-637 and *Colwellia psychrerythraea* GAB14E a gene cluster comparable to the one in MAG BB5 was identified

(Figure 6) and found to be largely conserved between the two species. BB5 additionally contains several other relevant genes, such as PutR regulator, stringent starvation proteins A and B, TonB dependent receptor, Zn/Fe binding domain protein, 1-pyrroline-4-hydroxy-2-carboxylate deaminase (dAminase) and a peptidyl-prolyl cis-trans isomerase PpiD (Rotamase).

Discussion

In this study, 59 high quality MAGs were reconstructed from microbes colonizing bone surface biofilms and from symbionts of the bone-eating worm *Osedax mucofloris*. Metabolic reconstruction revealed a complex, diverse and specialized community. Despite the differences in the bone material composition and structure between vertebrates (50), the major bacterial community compositions detected herein are in line with previously reported results using SSU rRNA gene profiling (33, 34). Our MAGs span at least 23 bacterial families and uncover a large potential for taxonomic novelty (over 50% according to genome-based taxonomy) from species up to class level in the bone microbiome. Interestingly, only genomes of gram-negative bacteria were reconstructed and despite gram-positive bacteria being widespread in the marine environment, they make up only minor portions of the metagenomes (1-1.2% of the reads affiliated to Firmicutes, Supplementary figure S1) (51). Moreover, they are known to carry out potentially relevant metabolic processes (thiotrophy, sulfidogenesis) (52, 53), are also capable of dealing with low pH conditions which are likely encountered during bone dissolution (54), and they possess high capacity for the secretion of hydrolytic enzymes (55). Therefore, these functions need to be accounted for by other gram-negative members of the microbial

316 communities. This study reveals the existence of a specialized bone-degrading microbiome in the
317 marine environment and starts to explore the enzymatic activities involved in the complete
318 demineralization of bone material.

319 **The role of *Osedax* endosymbionts in bone utilization**

320 *Osedax* species are known for their ability to acidify their environment via elevated expression
321 levels of vacuolar-H^+-ATPase (VHA) specifically in their root tissue and of carbonic anhydrase
322 in their whole body to dissolve calcium phosphate and access collagen and lipids from the bone
323 matrix (20). Miyamoto *et al.* found a high number of matrix metalloproteinases in the genome of
324 *Osedax japonicus* compared to other invertebrates, potentially assisting in digestion of collagen
325 and other proteins derived from bones (19). Two distinct bacterial endosymbiont genomes
326 belonging to the order Oceanospirillales have previously been sequenced, but their role in bone
327 degradation in the marine environment remained unclear (22). In this respect it is not surprising
328 that the bacterial fraction of the herein sequenced *Osedax mucofloris* metagenome is made up of
329 almost 27% Oceanospirillales affiliated reads, whereas the bone surface metagenome only
330 contains 1.9% reads of this order (Figure S1b). This relative difference confirms that the
331 methodological approach to minimize cross-contamination was successful and that the OB-
332 MAGs affiliated to Oceanospirilalles likely represent the symbiotic community of *Osedax*
333 *mucofloris* worms. The Oceanospirillales symbionts most likely benefit from the bone
334 degradation of their host, and therefore presumably do not reach high abundances in free-living
335 assemblages on the bone surface. Two MAGs belonging to the Oceanospirillales were identified
336 in the *Osedax*-associated metagenome, belonging to the genera *Neptunomonas* (OB1) and
337 *Amphritea* (OB2). Both genera are known to have an aerobic organotrophic lifestyle. As
338 hypothesized earlier for other *Osedax*-associated Oceanospirillales, their association with their

host might be casual and punctual, leading to a common benefit from a sudden nutrient bonanza (22, 25).

The degradative functions within the bone microbiome

Dissolution of inorganic compounds via a closed sulfur biogeochemical cycle

Free-living microbial communities, however, must deal with the same challenges as *Osedax* to access the nutrient rich, collagen-rich organic bone matrix and eventually the lipid-rich bone marrow by dissolving the hydroxyapatite. The association in large specialized consortia may be a beneficial strategy for achieving this. We hypothesize that sulfur-driven geomicrobiology (sulfate/thiosulfate/tetrathionate reduction and sulfide/sulfur/thiosulfate oxidation) is the major responsible factor for bone dissolution in the marine environment by free-living bacterial communities. Campylobacterales are one of the most abundant bacterial orders in the herein investigated metagenomes, in both the *Osedax*-associated metagenomes (OB) and the bone surface biofilms (BB) (Supplementary figure S2). Campylobacterales represent the most abundant group in terms of absolute read number, although it is the second largest taxon with reconstructed MAGs (Figure 1). Members of the Campylobacterales have previously been found to be associated with *Osedax*, albeit not as endosymbionts (25). The majority of retrieved Campylobacterales MAGs (14 in total) belong to different families of aerobic and facultative anaerobic (nitrate, manganese) sulfur-oxidizing bacteria (56, 57) (Thiovulaceae, Sulfurovaceae and Arcobacteraceae). Other aerobic/facultatively anaerobic (nitrate) sulfur oxidizing bacteria are also well represented in the order Beggiatoales (Gammaproteobacteria, 5 MAGs). *Beggiatoa*-like bacterial mats are commonly associated with whale falls (58) indicating an indifference regarding the bone type they dwell on. Sulfide oxidation produces elemental sulfur or sulfate (41,

45) while releasing protons and thereby leading to a drop in pH. This acidification mechanism has been linked to bone demineralization. The dissolution of the hydroxyapatite mineral exposes the organic matrix to enzymatic degradation (33, 34). Our hypothesis that this process is taking place here is supported by the elevated numbers of P-type ATPases (especially H^+-ATPases) (59, 60) found in the Beggiatoales MAGs and other unclassified γ-proteobacteria. Besides thiotrophy, that seems to be a major acid-producing mechanism in the microbial community, other mechanisms might also contribute significantly. In this respect, fermentative activities such as lactate dehydrogenases (*ldh*) that seem to correlate with high presence of proton pump ATPases are frequent in the MAGs. Moreover, a number of carbonic anhydrases (CA) were annotated, normally housekeeping genes involved in internal pH homeostasis and other processes (61). Here, the CAs were found to contain signal peptides for extracellular export (19 out of 94) and therefore could also be involved in acidification. Interestingly, 18 out of 19 identified CAs belong to the α-CA family and only one member of the β-CA family was found (Supplementary figure S4). The α-CA family is only found in gram negative bacteria, which is also the case here, and it is evolutionarily the youngest of the three bacterial CA families (40).

Besides a large number of SOB, eight MAGs related to SRB were identified that are affiliated to the families Desulfobulbaceae (also SOB), Desulfobacteraceae, Geopsychrobacteraceae and Desulfovibrionacaeae. Moreover, they are prevalently associated to the free-living community attached to the bone surface. Sulfate, tetrathionate or thiosulfate can serve as electron acceptors and/or donors and gene markers for all pathways are present in the metagenomes (Figure 2). Microbial sulfidogenesis on the bone surface or the surrounding sediments can feed the thiotrophic community and therefore accelerate the demineralization process. The generated sulfide is known to quickly react with iron, blackening the bone surfaces with insoluble iron

sulfide (62). In our incubation experiments, blackening is preferentially observed on the epiphysis, which is also where complex white/pink microbial mats are forming over time (supplementary figure S1B). However, SRB seem unable to degrade large complex molecules. This is supported by the lack of bone-degrading enzymes herein investigated, such as: S8/S53 peptidases, mannosidases, sialidases, fucosidases and α-galactosidases. SRB are likely dependent on the generation of simple organic compounds produced as metabolites by fermenters or aerobic organotrophic bacteria of the wider bone microbiome. The bone dissolution driven by sulfur geomicrobiology relies on other specialized members of the community to degrade the organic matrix and to fuel the acid generation.

Dissolution of organic compounds via peptidases, glucosidases and oxidases

Once the inorganic hydroxyapatite is removed an array of different enzymes is required to digest the various organic bone components. Bacteroidia appear to be especially remarkable in this respect and represent the third most abundant taxon. Eight high quality MAGs could be reconstructed, seven of them from the bone surface metagenome. Bacteroidia, and especially the family of Flavobacteriaceae, are known to be versatile degraders of polysaccharides like agar (63), chitin (64), ulvan (65), alginate (66), carrageen (67), cellulose and xylanose (68) and polypeptides like elastin (69), spongin (70) and others. The recently described Marinifilaceae family (71) includes isolates that are reported to present xylanase activity (72). Despite the discrepancy between abundance versus reconstructed genomes, the Bacteroidia MAGs appear to be the most versatile order of the investigated MAGs in respect to their richness in bone degrading enzymes (Figure 4), and all were predicted to possess the gelatin hydrolysis trait (Figure 3). They were also the only MAGs containing sialidases (COG4409) and α-galactosidases (Pfam16499) (Figure 4). Since most Bacteroidia MAGs were retrieved from the

surface associated microbiome, we assume that they play a pivotal role in the free-living community via the degradation of organic bone components.

Differential microbial colonization of the spongy cancellous bone tissue over the cortical compact bone has also been observed in the terrestrial environment and has been related to easier access to the red marrow (73). With complex microbial mats preferentially forming on the epiphysis of the long bones. Moreover, the epiphysis area is normally covered with hyaline cartilage (74) made of nonfibrous type II collagen and a sulfated-proteoglycan matrix rich in N-acetyl-galactosamine and glucuronic acid residues. This would explain the abundance of alpha-galactosidases, N-acetyl glucosaminidase and glucuronidases. Moreover, other groups such as Kiritimatiellales (PVC superphylum) are known marine anaerobic saccharolytic microbes specialized in degrading sulfated polymers that we find in this environment (75).

γ-proteobacteria - the collagen degraders

Peptidases and especially M9 collagenases are of special interest to bone and collagen degradation. The class γ-proteobacteria is comparatively enriched in these enzymes and it is the best represented class in the dataset, with 17 MAGs. Of particular interest are the MAGs affiliated to the order Enterobacterales (two MAGs of the families Kangiellaceae and one Alteromondaceae). They possess the gelatin hydrolysis trait (Figure 3, MAGs BB5, BB44 and OB12), have a high number of S1 and U32 peptidases, and are the only MAGs with M9 collagenases. The *Colwellia* MAG BB5 is particularly remarkable as it contains an entire gene cluster dedicated to collagen utilization (Figure 5A). The collagen degradation gene cluster comprises at least 15 different genes, including a M9 collagenase, a PepQ proline dipeptidase, an aminopeptidase YpdF, several transporters, epimerase, isomerases and others. The gene cluster

encodes nearly the entire pathway (missing genes are encoded elsewhere in the genome, like P5CDH) necessary to unwind and hydrolyze triple-helical collagen, transport and uptake of collagen oligopeptides into the cell and utilization of its main components, mainly hydroxyproline and proline, for energy production via the TCA cycle and/or the urea cycle or for polyamine biosynthesis (Figure 5B). This kind of functional condensation for collagen utilization has not been described before in *Colwellia* or elsewhere. Interestingly, *Colwellia* bacteria are also one partner in a dual extracellular symbiosis with sulfur-oxidizing bacteria in the mussel *Terua* sp. 'Guadelope', retrieved from a whale fall in the Antilles arc and supposedly involved in the utilization and uptake of bone components (76). A cluster of functionally related genes was found in the publicly available genomes of *Colwellia piezophila* and *Colwellia psychrerythraea*. However, the gene cluster described for MAG BB5 contains several supplementary features attributed to collagen utilization absent in the published genomes (Figure 6). Moreover, the gene cluster contains regulatory elements like the PutR regulator and stringent starvation proteins known to be activated under acid stress or amino acid starvation conditions in *Escherichia coli* (77). This supports our hypothesis that other members of the microbial community need to dissolve the bone calcium phosphate via acid secretion, before collagen and other organic bone compounds can be accessed.

Bone degradation – a complex microbial community effort

The marine bone microbiome is a complex assemblage of various bacterial classes that requires the synergistic action of many different interwoven enzymatic reactions to access the recalcitrant bone material for its nutritional resources. A scenario how we envision the orchestration of this complex process is depicted in Figure 7. The primary requirement in utilizing organic bone compounds is likely the dissolution of mineralized calcium phosphate (hydroxyapatite) by

acidification, which can potentially be performed via proton release by a versatile community of sulfur-oxidizing (SOB) γ-proteobacteria (mainly *Beggiatoa*-like), Campylobacterales (*Sulfurimonas*, *Sufurospirillum*, *Sulfurovum*), Desulfobubales and α-proteobacteria (Figure 7-I). This acidification via thiotrophy may be fueled by sulfur-reducing bacteria (SRB), like Desulfobacteraceae, Geopsychrobacteraceae, *Pseudodesulfovibrio*, creating a sulfur biogeochemical loop between SRB and SOB (Figure 7-II). Once the organic compounds (collagen, fatty acids, proteins, peptidoglycans) are accessible, the Bacteroidia (Flavobacteriaceae and Marinifiliaceae) and γ-proteobacteria (Alteromonadaceae and Kangiellaceae) may become the main protagonists (Figure 7 -III and IV). These Bacteroidia are especially rich in bone degrading enzymes, but importantly the γ-proteobacteria are the only members identified with M9 collagenases and *Colwellia* contains an entire gene cluster dedicated to collagen degradation (Figure 5). Herein we disentangled the potential functional roles of specialized members of the bone-degrading microbial community, which together make bone-derived nutrients accessible – not only to themselves, but also to generalists within the bone microbiome. We posit that Flavobacteriales and Enterobacterales are the most promising candidates for novel enzyme discovery, as they display the most versatile sets of bone degrading enzymes.

Materials and Methods

Sample collection

Four sets of turkey thigh bones and one bovine lower leg bone were deposited in Byfjorden (60,238185N; 5,181210E) close to Bergen, Norway, at a depth of 68 m in May 2016, incubated for nine months and retrieved using a small ROV (Table 1). The material was transported to the lab in Styrofoam boxes for either processing within two hours or for prolonged incubation in seawater aquaria. Bone surfaces were scraped for microorganisms and *Osedax mucofloris* specimens were extracted from the bone, preserved in storage solution (700 g/l ammonium sulfate, 20 mM sodium citrate and 25 mM EDTA, pH 5.2) and stored at -20 °C until further processing.

DNA extraction and sequencing

DNA was extracted from 10 to 50 mg sample using the Qiagen AllPrep DNA/RNA Mini Kit according to the manufacturer's instructions with cell lysis by a bead beating step in Lysing Matrix E tubes (MP Biomedicals) in a FastPrep homogenizer (MP Biomedicals) with a single cycle of 30s at a speed of 5500 rpm. The obtained metagenomic DNA was quantified and quality controlled using a NanoDrop2000 (ThermoFisher Scientific) and a Qubit fluorometer 3.0 (ThermoFisher Scientific). The metagenomic DNA was sequenced on an Illumina HiSeq4000 platform (150-bp paired-end reads) using Nextera library preparations at the Institute of Clinical Molecular Biology (IKMB), Kiel University, Germany.

SSU rRNA gene profiling

Illumina raw reads were quality trimmed and adapters were removed with Trimmomatic version 0.36 (78). The quality filtered reads were combined with respect to their sample source (either *Osedax*-associated or bone surface biofilms) and used for SSU rRNA gene profiling with phyloFlash version 3.3b1 (79). In brief, phyloFlash extracts all SSU rRNA gene containing reads from a metagenomic read dataset, assembles them using SPAdes (80) and calculates a taxonomic profile of the given metagenome. The phyloFlash pipeline was run using the –almosteverything option and operating at –taxlevel 2, to identify SSU rRNA gene reads up to an order level. The outputs for both metagenomic sample pools were compared using the phyloFlash_compare.pl script to generate barplots and heatmaps.

Metagenomic assembly, binning, taxonomic identification, ORF prediction and annotation

For each sample type (*Osedax mucofloris* and bone surface biofilm communities), the quality filtered metagenomic reads were co-assembled with SPAdes v3.12 (80) for kmers 21, 33, 55, 77 and 99, with the metaSPAdes-assembler option enabled. Binning was conducted on the resulting assemblies using the MetaWRAP pipeline (81). This pipeline combines three different implemented binning methods, CONCOCT (82), MaxBin2.0 (83) and metaBAT2 (84), to retrieve high quality MAGs. We only considered high-quality MAGs with >90% completeness and <10% redundancy for further analyses. CheckM was used for quality assessment of the assembles genomes (85), and GTDB-Tk version 0.1.3 (36) was used for taxonomic identification, coupled with an estimate of relative evolutionary divergence (RED) to their next common ancestor. RED is a normalization method to assign taxonomic ranks according to lineage-specific rates of evolution, based on branch lengths and internal nodes in relation to the last common ancestor calculated by GTDBTk. Alluvial diagrams based on taxonomic affiliations were designed with RAWgraphs (86). Open reading frames (ORF) of the obtained MAGs were

predicted with Prodigal version 2.6.3 (87). Predicted ORFs were annotated using eggNOG-mapper v1 (88) with eggNOG orthology data version 4.5 (89). Additionally, the MAGs were annotated and metabolic models were calculated using the RAST (Rapid Annotation using Subsystem Technology) server (90-92). The MAGs were further investigated for the presence or absence of major metabolic pathways and phenotypic microbial traits based on their genomic sequences using MEBS (Multigenomic Entropy Based Score) (37) and Traitar (39). Phylogenomic trees were drawn with iTOL (93, 94) and heatmaps were visualized with Heatmapper (95). Gene cluster maps were drawn with Gene Graphics (96). Signal peptides were predicted with SignalP-5.0 server usingnucleotide sequences to predict the presence of Sec/SPI, Tat/SPI and Sec/SPII signal peptides in a given sequence (97).

Enzyme profiling

Based on the organic composition of bone matrix, we hypothesized twelve enzyme families to be necessary for its degradation. Accordingly, the following enzymes were selected for in-depth studies: (i) M9 collagenases (pfam01752), S1 peptidases (COG0265), S8/S53 peptidases (pfam00082) and U32 proteases (COG0826) which hydrolyze peptide bonds in collagen and glycoproteins; (ii) sialidases (COG4409), β-d-glucuronidases (COG3250), β-N-acetyl-d-glucosaminidases (COG1472) which cleave glycosidic linkages, and (iii) α-N-acetylgalactosaminidases (COG0673), α-galactosidases (pfam16499), fucosidases (COG3669), mannosidases (COG0383) and cholesterol oxidases (COG2303) which degrade lipids such as cholesterol. One reference database for each of these families was generated using the NCBI repository, based on sequences from 287 M9 collagenases, 4453 S1 peptidases, 3237 S8/S53 peptidases, 3653 U32 proteases, 267 COG4409, 873 COG3250, 1274 COG1472, 6140 COG0673, 279 COG3669, 206 COG0383 and 1119 COG2303. The databases included the

closest protein homologs of all protein families of interest for bone-degradation, and at least one representative sequence from all taxonomic groups (containing such enzymes) was represented. The reference databases were used to generate Hidden Markov Model (HMM) profiles for each enzyme family with HMMER version 3.1b1 (98) using the *hmmbuild* option after an alignment of each sequence set was built with Clustal W version 2.1 (99). The MAGs were screened for the twelve enzyme families of interest using the generated HMM profiles using HMMer version 3.1b1 with the *hmmsearch* option and a bitscore threshold of 100.

Data availability

The raw sequencing reads have been deposited in the sequence read archive (SRA) of NCBI under the BioProject ID PRJNA606180 and with the BioSample accession numbers SAMN14086998 (A5), SAMN14087000 (A9), SAMN14087001 (A9n), SAMN14087003 (B4), SAMN14087005 (D1), SAMN14087006 (D2), SAMN14087007 (I1) and SAMN14087008 (I3).

Authors contributions

T.D., E.B., A.G.M. and G.E.K.B. developed the conceptual idea, conducted the sampling of the source material, contributed to content, reviewed and edited the manuscript. S.S.C., E.B. and M.F. identified enzymes of interest, constructed the reference databases and aided in result interpretation. E.B., B.S., S.F. and A.G.M. conducted bioinformatic analyses and E.B., B.S. and U.H. wrote the manuscript.

Acknowledgments

To the memory of Prof. Hans Tore Rapp and his effort on characterizing *Osedax mucofloris*. We acknowledge financial support of ERA-NET Marine Biotechnology (GA no.: 604814) funded under the FP7 ERA-NET scheme and nationally managed from the German Federal Ministry of Education and Research and Norwegian Research Council. M.F. acknowledges the Spanish Ministry support of Economythe grants PCIN-2017-078 (within the Marine Biotechnology ERA-NET) and BIO2017-85522-R from the Ministerio de Economía y Competitividad, Ministerio de Ciencia, Innovación y Universidades (MCIU), Agencia Estatal de Investigación (AEI), Fondo Europeo de Desarrollo Regional (FEDER) and Competiveness. Additional funding was received from the Norwegian Biodiversity Information Centre (PA 809116 knr. 47-14). We thank Hans T. Kleivdal for early developments of the concept. We thank Norilia AS for supplying bone residue material for the field work and ROV AS for providing underwater services during the deployment and sampling campaign. The authors acknowledge Kira S. Makarova at the National Center for Biotechnology Information (NCBI, Bethesda MD, USA) for help during the design of the reference database of enzyme families relevant to bone degradation.

582

583 **References**

584 1. Debashish G, Malay S, Barindra S, Joydeep M. 2005. Marine enzymes. Adv Biochem
585 Eng Biotechnol 96:189-218.
586 2. Imhoff JF, Labes A, Wiese J. 2011. Bio-mining the microbial treasures of the ocean: new
587 natural products. Biotechnol Adv 29:468-82.
588 3. Trincone A. 2011. Marine biocatalysts: enzymatic features and applications. Mar Drugs
589 9:478-99.
590 4. Adams MW, Perler FB, Kelly RM. 1995. Extremozymes: expanding the limits of
591 biocatalysis. Biotechnology (N Y) 13:662-8.
592 5. Aertsen A, Meersman F, Hendrickx ME, Vogel RF, Michiels CW. 2009. Biotechnology
593 under high pressure: applications and implications. Trends Biotechnol 27:434-41.
594 6. Cavicchioli R, Siddiqui KS, Andrews D, Sowers KR. 2002. Low-temperature
595 extremophiles and their applications. Curr Opin Biotechnol 13:253-61.
596 7. Feller G, Gerday C. 2003. Psychrophilic enzymes: hot topics in cold adaptation. Nat Rev
597 Microbiol 1:200-8.
598 8. Alcaide M, Tchigvintsev A, Martínez-Martínez M, Popovic A, Reva ON, Lafraya Á,
599 Bargiela R, Nechitaylo TY, Matesanz R, Cambon-Bonavita MA, Jebbar M, Yakimov
600 MM, Savchenko A, Golyshina OV, Yakunin AF, Golyshin PN, Ferrer M, Consortium M.
601 2015. Identification and characterization of carboxyl esterases of gill chamber-associated
602 microbiota in the deep-sea shrimp Rimicaris exoculata by using functional
603 metagenomics. Appl Environ Microbiol 81:2125-36.

9. Cowan D, Meyer Q, Stafford W, Muyanga S, Cameron R, Wittwer P. 2005. Metagenomic gene discovery: past, present and future. Trends Biotechnol 23:321-9.

10. Handelsman J. 2004. Metagenomics: application of genomics to uncultured microorganisms. Microbiol Mol Biol Rev 68:669-85.

11. Kennedy J, O'Leary ND, Kiran GS, Morrissey JP, O'Gara F, Selvin J, Dobson AD. 2011. Functional metagenomic strategies for the discovery of novel enzymes and biosurfactants with biotechnological applications from marine ecosystems. J Appl Microbiol 111:787-99.

12. Kodzius R, Gojobori T. 2015. Marine metagenomics as a source for bioprospecting. Mar Genomics 24 Pt 1:21-30.

13. Popovic A, Tchigvintsev A, Tran H, Chernikova TN, Golyshina OV, Yakimov MM, Golyshin PN, Yakunin AF. 2015. Metagenomics as a Tool for Enzyme Discovery: Hydrolytic Enzymes from Marine-Related Metagenomes. Adv Exp Med Biol 883:1-20.

14. Jørgensen BB, Boetius A. 2007. Feast and famine--microbial life in the deep-sea bed. Nat Rev Microbiol 5:770-81.

15. Naganuma T. 2000. [Microbes on the edge of global biosphere]. Biol Sci Space 14:323-31.

16. Sogin ML, Morrison HG, Huber JA, Mark Welch D, Huse SM, Neal PR, Arrieta JM, Herndl GJ. 2006. Microbial diversity in the deep sea and the underexplored "rare biosphere". Proc Natl Acad Sci U S A 103:12115-20.

17. Smith C, Baco A. 2003. Ecology of whale falls at the deep-sea floor, p 311-354. *In* Gibson R, Atkinson R (ed), Oceanography and Marine Biology: an Annual Review, vol 41. Taylor&Francis.

627 18. Rouse GW, Goffredi SK, Vrijenhoek RC. 2004. Osedax: bone-eating marine worms with
628 dwarf males. Science 305:668-71.
629 19. Miyamoto N, Yoshida MA, Koga H, Fujiwara Y. 2017. Genetic mechanisms of bone
630 digestion and nutrient absorption in the bone-eating worm Osedax japonicus inferred
631 from transcriptome and gene expression analyses. BMC Evol Biol 17:17.
632 20. Tresguerres M, Katz S, Rouse GW. 2013. How to get into bones: proton pump and
633 carbonic anhydrase in Osedax boneworms. Proc Biol Sci 280:20130625.
634 21. Higgs ND, Glover AG, Dahlgren TG, Little CT. 2011. Bone-boring worms:
635 characterizing the morphology, rate, and method of bioerosion by Osedax mucofloris
636 (Annelida, Siboglinidae). Biol Bull 221:307-16.
637 22. Goffredi SK, Yi H, Zhang Q, Klann JE, Struve IA, Vrijenhoek RC, Brown CT. 2014.
638 Genomic versatility and functional variation between two dominant heterotrophic
639 symbionts of deep-sea Osedax worms. ISME J 8:908-24.
640 23. Goffredi SK, Orphan VJ, Rouse GW, Jahnke L, Embaye T, Turk K, Lee R, Vrijenhoek
641 RC. 2005. Evolutionary innovation: a bone-eating marine symbiosis. Environ Microbiol
642 7:1369-78.
643 24. Goffredi SK, Johnson SB, Vrijenhoek RC. 2007. Genetic diversity and potential function
644 of microbial symbionts associated with newly discovered species of Osedax polychaete
645 worms. Appl Environ Microbiol 73:2314-23.
646 25. Verna C, Ramette A, Wiklund H, Dahlgren TG, Glover AG, Gaill F, Dubilier N. 2010.
647 High symbiont diversity in the bone-eating worm Osedax mucofloris from shallow
648 whale-falls in the North Atlantic. Environ Microbiol 12:2355-70.

649 26. Glover AG, Källström B, Smith CR, Dahlgren TG. 2005. World-wide whale worms? A
650 new species of Osedax from the shallow north Atlantic. Proc Biol Sci 272:2587-92.
651 27. Schander C, Rapp H, Dahlgren T. 2010. *Osedax mucofloris* (Polychaeta, Siboglinidae),
652 a bone-eating marine worm new to Norway. Fauna Norvegica 30:5-8.

653 28. Dahlgren T, Wiklund H, Källström B, Lundälv T, Smith C, Glover A. 2006. A shallow-
654 water whale-fall experiment in the North Atlantic. Cahiers De Biologie Marine 47:385-
655 389.
656 29. Robey PG. 2008. Noncollagenous bone matrix proteins, p 335-349. *In* Bilezikian JP,
657 Raisz LG, Martin JT (ed), Principles of bone biology, Third edition ed, vol Volume I.
658 Academic press.
659 30. Sato S, Rahemtulla F, Prince CW, Tomana M, Butler WT. 2009. Acidic glycoproteins
660 from bovine compact bone. Connective Tissue Research 14:51-64.
661 31. Kuboki Y, Watanabe T, Tazaki M, Taktta H. 1991. Comparative biochemistry of bone
662 matrix proteins in bovine and fish. *In* Suga S, Nakahara H (ed), Mechanisms and
663 phylogeny of mineralization in biological systems. Springer, Tokyo.
664 32. Shoulders MD, Raines RT. 2009. Collagen structure and stability. Annu Rev Biochem
665 78:929-58.
666 33. Vietti L, Bailey J, Ricci E. 2014. Insights into the microbial degradation of bone in
667 marine environments from rRNA gene sequencing of biofilms on lab-simulated carcass-
668 falls. The Paleontological Society Special Publications:120-121.
669 34. Vietti LA. 2014. Insights into the microbial degradation of bones from the marine
670 vertebrate fossil record: an experimental approach using interdisciplinary analyses. Ph.D.
671 dissertation. University of Minnesota, University of Minnesota Digital Conservancy.

672 35. Freitas RC, Marques HIF, Silva MACD, Cavalett A, Odisi EJ, Silva BLD, Montemor JE,
673 Toyofuku T, Kato C, Fujikura K, Kitazato H, Lima AOS. 2019. Evidence of selective
674 pressure in whale fall microbiome proteins and its potential application to industry. Mar
675 Genomics 45:21-27.
676 36. Parks DH, Chuvochina M, Waite DW, Rinke C, Skarshewski A, Chaumeil PA,
677 Hugenholtz P. 2018. A standardized bacterial taxonomy based on genome phylogeny
678 substantially revises the tree of life. Nat Biotechnol 36:996-1004.
679 37. De Anda V, Zapata-Peñasco I, Poot-Hernandez AC, Eguiarte LE, Contreras-Moreira B,
680 Souza V. 2017. MEBS, a software platform to evaluate large (meta)genomic collections
681 according to their metabolic machinery: unraveling the sulfur cycle. Gigascience 6:1-17.
682 38. Müller AL, Kjeldsen KU, Rattei T, Pester M, Loy A. 2015. Phylogenetic and
683 environmental diversity of DsrAB-type dissimilatory (bi)sulfite reductases. ISME J
684 9:1152-65.
685 39. Weimann A, Mooren K, Frank J, Pope PB, Bremges A, McHardy AC. 2016. From
686 Genomes to Phenotypes: Traitar, the Microbial Trait Analyzer. mSystems 1.
687 40. Capasso C, Supuran CT. 2015. An overview of the alpha-, beta- and gamma-carbonic
688 anhydrases from Bacteria: can bacterial carbonic anhydrases shed new light on evolution
689 of bacteria? J Enzyme Inhib Med Chem 30:325-32.
690 41. Yamamoto M, Takai K. 2011. Sulfur metabolisms in epsilon- and gamma-proteobacteria
691 in deep-sea hydrothermal fields. Front Microbiol 2:192.
692 42. Muyzer G, Stams AJ. 2008. The ecology and biotechnology of sulphate-reducing
693 bacteria. Nat Rev Microbiol 6:441-54.

694 43. Barton LL, Fauque GD. 2009. Biochemistry, physiology and biotechnology of sulfate-
695 reducing bacteria. Adv Appl Microbiol 68:41-98.
696 44. Kruse S, Goris T, Westermann M, Adrian L, Diekert G. 2018. Hydrogen production by
697 Sulfurospirillum species enables syntrophic interactions of Epsilonproteobacteria. Nat
698 Commun 9:4872.
699 45. Schulz HN, Jorgensen BB. 2001. Big bacteria. Annu Rev Microbiol 55:105-37.
700 46. Gevertz D, Telang AJ, Voordouw G, Jenneman GE. 2000. Isolation and characterization
701 of strains CVO and FWKO B, two novel nitrate-reducing, sulfide-oxidizing bacteria
702 isolated from oil field brine. Appl Environ Microbiol 66:2491-501.
703 47. Poser A, Vogt C, Knöller K, Ahlheim J, Weiss H, Kleinsteuber S, Richnow HH. 2014.
704 Stable sulfur and oxygen isotope fractionation of anoxic sulfide oxidation by two
705 different enzymatic pathways. Environ Sci Technol 48:9094-102.
706 48. Trojan D, Schreiber L, Bjerg JT, Bøggild A, Yang T, Kjeldsen KU, Schramm A. 2016. A
707 taxonomic framework for cable bacteria and proposal of the candidate genera
708 Electrothrix and Electronema. Syst Appl Microbiol 39:297-306.
709 49. Pfeffer C, Larsen S, Song J, Dong M, Besenbacher F, Meyer RL, Kjeldsen KU, Schreiber
710 L, Gorby YA, El-Naggar MY, Leung KM, Schramm A, Risgaard-Petersen N, Nielsen
711 LP. 2012. Filamentous bacteria transport electrons over centimetre distances. Nature
712 491:218-21.
713 50. Aerssens J, Boonen S, Lowet G, Dequeker J. 1998. Interspecies differences in bone
714 composition, density, and quality: potential implications for in vivo bone research.
715 Endocrinology 139:663-70.

716 51. Gontang EA, Fenical W, Jensen PR. 2007. Phylogenetic diversity of gram-positive
717 bacteria cultured from marine sediments. Appl Environ Microbiol 73:3272-82.
718 52. Teske A, Brinkhoff T, Muyzer G, Moser DP, Rethmeier J, Jannasch HW. 2000. Diversity
719 of thiosulfate-oxidizing bacteria from marine sediments and hydrothermal vents. Appl
720 Environ Microbiol 66:3125-33.
721 53. Leloup J, Fossing H, Kohls K, Holmkvist L, Borowski C, Jørgensen BB. 2009. Sulfate-
722 reducing bacteria in marine sediment (Aarhus Bay, Denmark): abundance and diversity
723 related to geochemical zonation. Environ Microbiol 11:1278-91.
724 54. Cotter PD, Hill C. 2003. Surviving the acid test: responses of gram-positive bacteria to
725 low pH. Microbiol Mol Biol Rev 67:429-53, table of contents.
726 55. Anné J, Economou A, Bernaerts K. 2017. Protein Secretion in Gram-Positive Bacteria:
727 From Multiple Pathways to Biotechnology. Curr Top Microbiol Immunol 404:267-308.
728 56. Lastovica A, On S, Zhang L. 2014. The family *Campylobacteraceae*, p 307-335. *In*
729 Rosenburg E, DeLong E, Lory S, Stackebrandt E, Thompson F (ed), The Prokaryotes.
730 Springer.
731 57. Takai K, Campbell BJ, Cary SC, Suzuki M, Oida H, Nunoura T, Hirayama H, Nakagawa
732 S, Suzuki Y, Inagaki F, Horikoshi K. 2005. Enzymatic and genetic characterization of
733 carbon and energy metabolisms by deep-sea hydrothermal chemolithoautotrophic isolates
734 of Epsilonproteobacteria. Appl Environ Microbiol 71:7310-20.
735 58. Deming JW, Reysenbach AL, Macko SA, Smith CR. 1997. Evidence for the microbial
736 basis of a chemoautotrophic invertebrate community at a whale fall on the deep seafloor:
737 bone-colonizing bacteria and invertebrate endosymbionts. Microsc Res Tech 37:162-70.
738 59. Palmgren MG, Nissen P. 2011. P-type ATPases. Annu Rev Biophys 40:243-66.

739 60. Morth JP, Pedersen BP, Buch-Pedersen MJ, Andersen JP, Vilsen B, Palmgren MG,
740 Nissen P. 2011. A structural overview of the plasma membrane Na+,K+-ATPase and H+-
741 ATPase ion pumps. Nat Rev Mol Cell Biol 12:60-70.
742 61. Supuran CT, Capasso C. 2017. An Overview of the Bacterial Carbonic Anhydrases.
743 Metabolites 7.
744 62. Vietti L, Bailey J, Fox D, Rogers R. 2015. Rapid formation of framboidal sulfides on
745 bone surfaces from a simulated marine carcass fall. PALAIOS 30:327-334.
746 63. Naretto A, Fanuel M, Ropartz D, Rogniaux H, Larocque R, Czjzek M, Tellier C, Michel
747 G. 2019. The agar-specific hydrolase. J Biol Chem 294:6923-6939.
748 64. Nedashkovskaya OI, Kim SG, Stenkova AM, Kukhlevskiy AD, Zhukova NV, Mikhailov
749 VV. 2018. Aquimarina algiphila sp. nov., a chitin degrading bacterium isolated from the
750 red alga Tichocarpus crinitus. Int J Syst Evol Microbiol 68:892-898.
751 65. Konasani VR, Jin C, Karlsson NG, Albers E. 2018. A novel ulvan lyase family with
752 broad-spectrum activity from the ulvan utilisation loci of Formosa agariphila KMM 3901.
753 Sci Rep 8:14713.
754 66. Li S, Wang L, Chen X, Zhao W, Sun M, Han Y. 2018. Cloning, Expression, and
755 Biochemical Characterization of Two New Oligoalginate Lyases with Synergistic
756 Degradation Capability. Mar Biotechnol (NY) 20:75-86.
757 67. Shen J, Chang Y, Chen F, Dong S. 2018. Expression and characterization of a κ-
758 carrageenase from marine bacterium Wenyingzhuangia aestuarii OF219: A
759 biotechnological tool for the depolymerization of κ-carrageenan. Int J Biol Macromol
760 112:93-100.

761 68. Tan H, Miao R, Liu T, Yang L, Yang Y, Chen C, Lei J, Li Y, He J, Sun Q, Peng W, Gan
762 B, Huang Z. 2018. A bifunctional cellulase-xylanase of a new Chryseobacterium strain
763 isolated from the dung of a straw-fed cattle. Microb Biotechnol 11:381-398.
764 69. Rochat T, Pérez-Pascual D, Nilsen H, Carpentier M, Bridel S, Bernardet JF, Duchaud E.
765 2019. Identification of a Novel Elastin-Degrading Enzyme from the Fish Pathogen. Appl
766 Environ Microbiol 85.
767 70. Choi KD, Lee GE, Park JS. 2018. Aquimarina spongiicola sp. nov., isolated from
768 spongin. Int J Syst Evol Microbiol 68:990-994.
769 71. Iino T, Mori K, Itoh T, Kudo T, Suzuki K, Ohkuma M. 2014. Description of Mariniphaga
770 anaerophila gen. nov., sp. nov., a facultatively aerobic marine bacterium isolated from
771 tidal flat sediment, reclassification of the Draconibacteriaceae as a later heterotypic
772 synonym of the Prolixibacteraceae and description of the family Marinifilaceae fam. nov.
773 Int J Syst Evol Microbiol 64:3660-7.
774 72. Han Z, Shang-Guan F, Yang J. 2019. Molecular and Biochemical Characterization of a
775 Bimodular Xylanase From. Front Microbiol 10:1507.
776 73. Emmons A, Mundorff A, Keenan S, Davoren J, Andronowski J, Carter D, DeBruyn J.
777 2019. Patterns of microbial colonization of human bone from surface-decomposed
778 remains. bioRxiv 664482.
779 74. Robey P. 2002. Bone matrix proteoglycans and glycoproteins. *In* Bilezikian J, Raisz L,
780 Rodan G (ed), Principles of bone biology, 2nd Edition ed. Elsevier.
781 75. van Vliet DM, Palakawong Na Ayudthaya S, Diop S, Villanueva L, Stams AJM,
782 Sánchez-Andrea I. 2019. Anaerobic Degradation of Sulfated Polysaccharides by Two
783 Novel. Front Microbiol 10:253.

784 76. S D, O G. 2016. Colwellia and sulfur-oxidizing bacteria: An unusual dual symbiosis in a
785 Terua mussel (Mytilidae: Bathymodiolinae) from whale falls in the Antilles arc. Deep
786 Sea Research Part I 115:112-122.
787 77. Hansen AM, Qiu Y, Yeh N, Blattner FR, Durfee T, Jin DJ. 2005. SspA is required for
788 acid resistance in stationary phase by downregulation of H-NS in Escherichia coli. Mol
789 Microbiol 56:719-34.
790 78. Bolger AM, Lohse M, Usadel B. 2014. Trimmomatic: a flexible trimmer for Illumina
791 sequence data. Bioinformatics 30:2114-20.
792 79. Gruber-Vodicka HR, Seah BKB, Pruesse E. 2019. phyloFlash - Rapid SSU rRNA
793 profiling and targeted assembly from metagenomes. bioRxiv.
794 80. Bankevich A, Nurk S, Antipov D, Gurevich AA, Dvorkin M, Kulikov AS, Lesin VM,
795 Nikolenko SI, Pham S, Prjibelski AD, Pyshkin AV, Sirotkin AV, Vyahhi N, Tesler G,
796 Alekseyev MA, Pevzner PA. 2012. SPAdes: a new genome assembly algorithm and its
797 applications to single-cell sequencing. J Comput Biol 19:455-77.
798 81. Uritskiy GV, DiRuggiero J, Taylor J. 2018. MetaWRAP-a flexible pipeline for genome-
799 resolved metagenomic data analysis. Microbiome 6:158.
800 82. Alneberg J, Bjarnason BS, de Bruijn I, Schirmer M, Quick J, Ijaz UZ, Lahti L, Loman
801 NJ, Andersson AF, Quince C. 2014. Binning metagenomic contigs by coverage and
802 composition. Nat Methods 11:1144-6.
803 83. Wu YW, Simmons BA, Singer SW. 2016. MaxBin 2.0: an automated binning algorithm
804 to recover genomes from multiple metagenomic datasets. Bioinformatics 32:605-7.

805 84. Kang DD, Li F, Kirton E, Thomas A, Egan R, An H, Wang Z. 2019. MetaBAT 2: an
806 adaptive binning algorithm for robust and efficient genome reconstruction from
807 metagenome assemblies. PeerJ 7:e7359.
808 85. Parks DH, Imelfort M, Skennerton CT, Hugenholtz P, Tyson GW. 2015. CheckM:
809 assessing the quality of microbial genomes recovered from isolates, single cells, and
810 metagenomes. Genome Res 25:1043-55.
811 86. Mauri M, Elli, T., Caviglia, G., Uboldi, G., & Azzi, M. RAWGraphs: A Visualisation
812 Platform to Create Open Outputs., p. *In* (ed),
813 87. Hyatt D, Chen GL, Locascio PF, Land ML, Larimer FW, Hauser LJ. 2010. Prodigal:
814 prokaryotic gene recognition and translation initiation site identification. BMC
815 Bioinformatics 11:119.
816 88. Huerta-Cepas J, Forslund K, Coelho LP, Szklarczyk D, Jensen LJ, von Mering C, Bork P.
817 2017. Fast Genome-Wide Functional Annotation through Orthology Assignment by
818 eggNOG-Mapper. Mol Biol Evol 34:2115-2122.
819 89. Huerta-Cepas J, Szklarczyk D, Forslund K, Cook H, Heller D, Walter MC, Rattei T,
820 Mende DR, Sunagawa S, Kuhn M, Jensen LJ, von Mering C, Bork P. 2016. eggNOG 4.5:
821 a hierarchical orthology framework with improved functional annotations for eukaryotic,
822 prokaryotic and viral sequences. Nucleic Acids Res 44:D286-93.
823 90. Aziz RK, Bartels D, Best AA, DeJongh M, Disz T, Edwards RA, Formsma K, Gerdes S,
824 Glass EM, Kubal M, Meyer F, Olsen GJ, Olson R, Osterman AL, Overbeek RA, McNeil
825 LK, Paarmann D, Paczian T, Parrello B, Pusch GD, Reich C, Stevens R, Vassieva O,
826 Vonstein V, Wilke A, Zagnitko O. 2008. The RAST Server: rapid annotations using
827 subsystems technology. BMC Genomics 9:75.

828 91. Brettin T, Davis JJ, Disz T, Edwards RA, Gerdes S, Olsen GJ, Olson R, Overbeek R,
829 Parrello B, Pusch GD, Shukla M, Thomason JA, Stevens R, Vonstein V, Wattam AR,
830 Xia F. 2015. RASTtk: a modular and extensible implementation of the RAST algorithm
831 for building custom annotation pipelines and annotating batches of genomes. Sci Rep
832 5:8365.
833 92. Overbeek R, Olson R, Pusch GD, Olsen GJ, Davis JJ, Disz T, Edwards RA, Gerdes S,
834 Parrello B, Shukla M, Vonstein V, Wattam AR, Xia F, Stevens R. 2014. The SEED and
835 the Rapid Annotation of microbial genomes using Subsystems Technology (RAST).
836 Nucleic Acids Res 42:D206-14.
837 93. Letunic I, Bork P. 2007. Interactive Tree Of Life (iTOL): an online tool for phylogenetic
838 tree display and annotation. Bioinformatics 23:127-8.
839 94. Letunic I, Bork P. 2019. Interactive Tree Of Life (iTOL) v4: recent updates and new
840 developments. Nucleic Acids Res 47:W256-W259.
841 95. Babicki S, Arndt D, Marcu A, Liang Y, Grant JR, Maciejewski A, Wishart DS. 2016.
842 Heatmapper: web-enabled heat mapping for all. Nucleic Acids Res 44:W147-53.
843 96. Harrison KJ, Crécy-Lagard V, Zallot R. 2018. Gene Graphics: a genomic neighborhood
844 data visualization web application. Bioinformatics 34:1406-1408.
845 97. Almagro Armenteros JJ, Tsirigos KD, Sønderby CK, Petersen TN, Winther O, Brunak S,
846 von Heijne G, Nielsen H. 2019. SignalP 5.0 improves signal peptide predictions using
847 deep neural networks. Nat Biotechnol 37:420-423.
848 98. Eddy SR. 2011. Accelerated Profile HMM Searches. PLoS Comput Biol 7:e1002195.

849 99. Larkin MA, Blackshields G, Brown NP, Chenna R, McGettigan PA, McWilliam H,
850 Valentin F, Wallace IM, Wilm A, Lopez R, Thompson JD, Gibson TJ, Higgins DG.
851 2007. Clustal W and Clustal X version 2.0. Bioinformatics 23:2947-8.

852

853

854

855

856

857

858

859

860

861

862

863

864

865

866

867

868 **Tables:**

869 **Table 1:** Metagenome sampling information and number of retrieved metagenome assembled

870 genomes (MAG).

Sample	Sample type	Bone type, organism	Collection dates	Sampling location (GPS)	High quality MAGs
A5 A9 A9n B4	*Osedax mucofloris*	Femur, turkey (*Meleagris gallopavo*)	08.01.2017 08.02.2017 08.02.2017 14.04.2017	Byfjorden, Bergen, Norway (60,238185N; 5,181210E)	15 (OB)
D1 D2 I1 I3	Bone surface biofilm communities	Tibia, cow (*Bos taurus*)	02.2017 11.12.2017 27.01.2017 11.12.2017		44 (BB)

871

872 **Table 2:** Taxonomic affiliation of MAGs according to Parks *et al.* (2018) and taxonomic novelty

873 identified by RED (*) (36).

MAG	Phylum	Class	Order	Family	Genus
BB1	Planctomycetota*	-	-	-	-
BB2	Proteobacteria	γ-proteobacteria	Beggiatoales*	-	-
BB3	Proteobacteria	γ-proteobacteria	Beggiatoales	Beggiatoaceae*	-
BB4	Proteobacteria	γ-proteobacteria*	-	-	-
BB5	Proteobacteria	γ-proteobacteria	Enterobacterales	Alteromonadaceae	Colwellia
BB6	Proteobacteria	α-proteobacteria	Rhizobiales*	-	-
BB7	Spirochaetota	Spirochaetia	Spirochaetales	Spirochaetaceae*	-
BB8	Campylobacterota	Camylobacteria	Campylobacterales	-	-
BB9	Campylobacterota	Camylobacteria	Campylobacterales	Sulfurovaceae	Sulfurovum
BB10	Campylobacterota	Camylobacteria	Campylobacterales	Thiovulaceae*	-
BB11	Campylobacterota	Camylobacteria	Campylobacterales	Thiovulaceae	Sulfurimonas
BB12	Fermentibacterota	Fermentibacteria	Fermentibacterales	Fermentibacteraceae*	-
BB13	Desulfobacterota	Desulfobulbia	Desulfobulbales	Desulfobulbaceae*	-
BB14	Campylobacterota	Camylobacteria	Campylobacterales	Sulfurovaceae*	-
BB15	Campylobacterota	Camylobacteria	Campylobacterales	Sulfurospirillaceae	Sulfurospirillum

BB16	Proteobacteria	γ-proteobacteria	Beggiatoales	Beggiatoaceae	Marithrix*
BB17	Bacteroidota	Bacteroidia	Flavobacteriales	Ichthyobacteriaceae*	-
BB18	Krumholzibacteriota	Krumholzibacteria*	-	-	-
BB19	Proteobacteria	γ-proteobacteria	Pseudomonadales	Hahellaceae*	-
BB20	Proteobacteria	γ-proteobacteria	Beggiatoales*	-	-
BB21	Desulfuromonadota	Desulfuromonadia	Desulfuromonadales	Geopsychrobacteraceae	Desulfuromusa
BB22	Bacteroidota	Bacteroidia	Bacteroidales*	-	-
BB23	Bacteroidota	Bacteroidia	Flavobacteriales	Flavobacteriaceae	Winogradskyella
BB24	Bacteroidota	Bacteroidia	Flavobacteriales	Flavobacteriaceae*	-
BB25	Desulfuromonadota	Desulfuromonadia	Desulfuromonadales	Geopsychrobacteraceae	Desulfuromusa
BB26	Campylobacterota	Camylobacteria	Campylobacterales	Thiovulaceae*	-
BB27	Desulfuromonadota	Desulfuromonadia	Desulfuromonadales	Geopsychrobacteraceae*	-
BB28	Campylobacterota	Camylobacteria	Campylobacterales	Arcobacteraceae*	-
BB29	Bacteroidota	Bacteroidia	Bacteroidales	Marinifilaceae	-
BB30	Campylobacterota	Camylobacteria	Campylobacterales	Arcobacteraceae	Arcobacter
BB31	Proteobacteria	γ-proteobacteria	Beggiatoales*	-	-
BB32	Proteobacteria	γ-proteobacteria	Xanthomonadales	Marinicellaceae*	-
BB33	Proteobacteria	α-proteobacteria	Rhodobacterales	Rhodobacteraceae	Lentibacter*
BB34	Proteobacteria	γ-proteobacteria*	-	-	-
BB35	Bacteroidota	Bacteroidia	Flavobacteriales	Flavobacteriaceae	-
BB36	Proteobacteria	γ-proteobacteria*			
BB37	Proteobacteria	γ-proteobacteria	Pseudomonadales	Halieaceae*	-
BB38	Chloroflexota	Anaerolineae	Anearolineales*	-	-
BB39	Krumholzibacteriota	Krumholzibacteria*	-	-	-
BB40	Desulfobacterota	Desulfobacteria	Desulfobacterales	Desulfobacteraceae	-
BB41	Campylobacterota	Camylobacteria	Campylobacterales	Sulfurovaceae*	-
BB42	Bacteroidota	Bacteroidia	Flavobacteriales	Flavobacteriaceae	Maribacter*
BB43	Verrucomicrobiota	Kiritimatiellae	Kiritimatiellales*	-	-
BB44	Proteobacteria	γ-proteobacteria	Enterobacterales	Kangiellaceae*	-
OB1	Proteobacteria	γ-proteobacteria	Pseudomonadales	Nitrincolaceae	Neptunomonas
OB2	Proteobacteria	γ-proteobacteria	Pseudomonadales	Nitrincolaceae	Amphritea
OB3	Desulfobacterota	Desulfovibrionia	Desulfovibrionales	Desulfovibrionaceae	Pseudodesulfovibrio
OB4	Proteobacteria	α-proteobacteria	Sphingomonadales	Emcibacteraceae*	-
OB5	Campylobacterota	Camylobacteria	Campylobacterales	Thiovulaceae	Sulfurimonas
OB6	Proteobacteria	γ-proteobacteria*	-	-	-
OB7	Campylobacterota	Camylobacteria	Campylobacterales	Arcobacteraceae	Arcobacter
OB8	Campylobacterota	Camylobacteria	Campylobacterales	Thiovulaceae	Sulfurimonas
OB9	Proteobacteria	α-proteobacteria	Rhodobacterales	Rhodobacteraceae	-
OB10	Verrucomicrobiota	Kiritimatiellae	Kiritimatiellales*	-	-
OB11	Campylobacterota	Camylobacteria	Campylobacterales	Sulfurospirillaceae	Sulfurospirillum
OB12	Proteobacteria	γ-proteobacteria	Enterobacterales	Kangiellaceae*	-
OB13	Bacteroidota	Bacteroidia	Bacteroidales	Marinifilaceae	Labilibaculum*
OB14	Desulfobacterota	Desulfobacteria	Desulfobacterales	Desulfobacteraceae	-
OB15	Proteobacteria	α-proteobacteria*	-	-	-

874

875 **Figures**

876 **Figure 1:** Alluvial diagram of the taxonomic affiliation of all 59 obtained high quality MAGs,
877 spanning 11 phyla, 14 classes, 19 orders and at least 23 families. 37 out of 59 MAGs were
878 identified as taxonomically novel as determined by their relative evolutionary divergence (RED)
879 to their closest common ancestor. The taxonomic affiliation was inferred with GTDBTk (36) and
880 visualized with RAWGraphs (86).

881 **Figure 2:** Whole genome metabolic pathway comparison. Analysis was done with MEBS (37)
882 and MAGs are phylogenetically grouped according to GTDBTk pipeline (36). The color
883 gradients are explained next to the heatmaps. The heatmap shows the presence of marker genes
884 or completeness of different metabolic systems within the MAGs.

885 **Figure 3:** Taxonomic relationship, gelatin hydrolysis analysis, SRB and SOB within the surface
886 communities (Biofilm) and *Osedax* metagenomes. MAGs are displayed with the deepest
887 taxonomic classification obtained. Bacterial clades predicted to encode the gelatin hydrolysis
888 trait are depicted in green according to analysis with Traitar (39), SRB are encircled in blue and
889 SOB in orange.

890 **Figure 4:** Presence of putative bone degrading enzymes in extracted MAGs. A) Abundance
891 heatmap of the 12 investigated enzyme classes in the 59 high quality MAGs. The MAGs are
892 arranged according to taxonomic affiliation. The absolute abundances of each enzyme class are
893 depicted in the diagram on top of the heatmap. C) Percental distribution of all 722 identified
894 enzymes according to their enzyme class.

Figure 5: Collagen utilization in MAG BB5. A) Gene cluster in BB5, comprising 15 genes for collagen utilization, each color-coded respective to its functional group: orange for collagen hydrolysis, blue for uptake and transport, green for proline (Pro) utilization, ocher for hydroxyproline (Hyp) utilization and brown for unknown function. A light box is indicative of a predicted signal-peptide for secretion. B) Metabolic prediction model for functional collagen utilization in *Colwellia* BB5. Arrows and genes are color coded in the same functional groups as in A. Gray dotted arrows indicate a connection to a major metabolic pathway. Intermediate abbreviations: P4C (1-pyrroline 4-hydroxy-2-carboxylate), KGSA (alpha-ketoglutarate semialdehyde), KG (alpha-ketoglutarate), P5C (1-pyrroline-5-carboxylate). Enzyme abbreviations: D-aa dHase (D-hydroxyproline dehydrogenase), dAminase (pyrroline-4-hydroxy-2-carboxylate deaminase), di-oxo dHase (KGSA dehydrogenase), P5CR/ornithine dAminase (bifunctional 1-pyrroline-5-carboxylate reductase/ornithine cyclodeaminase), PRODH (proline dehydrogenase), P5CDH (pyrroline-5-carboxylate dehydrogenase).

Figure 6: Conservation between M9 collagen degradation gene clusters in *Colwellia psychrerythraea* GAB14E, *Colwellia piezophila* ATCC BAA-637 and the MAG *Colwellia* BB5 drawn at scale. dHase, dehydrogenase; PPIase, peptidyl-prolyl cis trans isomerase; Hyp, D-aa, dAminase etc. Color coding and gene names are indicated.

Figure 7: Hypothesis of the interplay in the marine bone microbiome and degradome. (I) Sulfur-oxidizing bacteria (SOB, shown with a halo) convert elemental sulfur and H_2S into sulfate and protons that lead to an acidification and therefore bone demineralization. (II) Sulfate reducing (SRB, green) and sulfur disproportioning bacteria produce H_2S from sulfate. (III) Enterobacterales and other especially γ-proteobatceria secret collagenases to degrade collagen. (IV) Bacteroidia and other bacteria secret gylcosidases and other enzymes to hydrolyze the

organic bone components (glycosides, esters, lipids). This exemplifies a bone demineralization loop that fuels itself as long as sulfur is available and degrades the organic bone components in the process.

936

937 **Supplementary material**

938 **Supplementary tables**

939 **Supplementary table S1:** MAG sequence data. All MAGs labeled 'OB' were retrieved from

940 **Osedax samples and all MAGs labeled with 'BB' from bone surface biofilms.**

MAG	Genome size [Mbp]	Longest contig	N50	No. of contigs	Predicted genes	GC content	No. of bone-degrading Enzymes
BB_1	4.68	155 kbp	429 kbp	38	3723	44.50%	24
BB_2	4.18	853 kbp	248 kbp	108	3538	44.10%	13
BB_3	4.65	75 kbp	23 kbp	362	4126	37.70%	11
BB_4	5.18	1.05 Mbp	198 kbp	68	4705	38.80%	13
BB_5	3.26	82 kbp	13 kbp	395	3018	36.10%	16
BB_6	2.77	72 kbp	19 kbp	244	2783	40.10%	10
BB_7	4.87	78 kbp	15 kbp	489	4636	40.10%	22
BB_8	3.08	89 kbp	18 kbp	413	3332	32.90%	11
BB_9	2.16	126 kbp	36 kbp	159	2259	36.80%	5
BB_10	3.01	137 kbp	35 kbp	142	2950	36.20%	11
BB_11	2.39	21 kbp	3 kbp	809	2958	35.40%	6
BB_12	3.24	329 kbp	141 kbp	127	2929	45.10%	10
BB_13	4.24	16 kbp	3 kbp	1688	4778	48%	16
BB_14	2.32	74 kbp	33 kbp	103	2265	34.20%	8
BB_15	2.68	415 kbp	191 kbp	33	2695	30.70%	5
BB_16	3.09	481 kbp	237 kbp	22	2867	34.10%	13
BB_17	3.64	81 kbp	16 kbp	327	3171	32.30%	13
BB_18	4.43	267 kbp	114 kbp	176	3652	52.60%	23
BB_19	4.07	273 kbp	132 kbp	88	3778	41.30%	13
BB_20	4.49	73 kbp	19 kbp	338	3725	37.90%	13
BB_21	2.89	145 kbp	51 kbp	186	2812	44.40%	8
BB_22	5.23	124 kbp	28 kbp	294	4210	34.20%	32
BB_23	3.72	128 kbp	30 kbp	190	3427	23.40%	9
BB_24	4.64	57 kbp	16 kbp	582	4438	31.30%	58
BB_25	3.31	211 kbp	67 kbp	118	3069	44.30%	8
BB_26	3.59	77 kbp	23 kbp	242	3547	44.60%	8
BB_27	2.58	39 kbp	9 kbp	514	2602	43.10%	9

BB_28	3.02	103 kbp	27 kbp	187	3056	26.30%	4
BB_29	4.16	122 kbp	21 kbp	304	3375	34.40%	21
BB_30	1.99	35 kbp	9 kbp	292	2109	25.80%	4
BB_31	5.34	141 kbp	35 kbp	263	4342	45.30%	15
BB_32	3.62	326 kbp	117 kbp	52	3061	35.20%	14
BB_33	3.25	137 kbp	77 kbp	74	3319	56.80%	9
BB_34	4.87	115 kbp	31 kbp	302	4339	38.20%	9
BB_35	3.13	1.08 Mbp	834 kbp	7	2773	31.80%	12
BB_36	4.29	149 kbp	54 kbp	138	3907	39.10%	9
BB_37	3.94	120 kbp	29 kbp	353	3831	51.50%	11
BB_38	3.62	242 kbp	62 kbp	144	3260	44.20%	14
BB_39	4.06	50 kbp	7 kbp	814	3832	59.10%	17
BB_40	6.73	296 kbp	113kbp	106	5886	45.10%	0
BB_41	2.54	64 kbp	13 kbp	288	2631	32.90%	7
BB_42	3.59	118 kbp	30 kbp	186	3352	33.10%	23
BB_43	3.69	317 kbp	19 kbp	330	3767	49.10%	10
BB_44	4.03	21 kbp	5 kbp	985	4077	40.20%	17
OB_1	4.21	150 kbp	53 kbp	143	3949	43.10%	13
OB_2	4.15	563 kbp	111 kbp	53	3804	47.20%	14
OB_3	3.96	2.09 Mbp	2.09 Mbp	150	3665	48.70%	16
OB_4	2.73	66.9 kbp	15 kbp	778	2962	38.90%	4
OB_5	2.05	107 kbp	50 kbp	81	2113	31.90%	5
OB_6	3.88	180 kbp	68 kbp	100	3643	39.10%	11
OB_7	1.78	24 kbp	5 kbp	586	1916	26.10%	2
OB_8	2.92	106 kbp	17 kbp	269	3159	31.60%	7
OB_9	3.13	432 kbp	190 kbp	55	3181	55.10%	6
OB_10	3	55 kbp	14 kbp	316	2910	48.60%	10
OB_11	2.69	324 kbp	101 kbp	212	2676	30.50%	5
OB_12	4.68	59 kbp	21 kbp	361	4128	39.90%	22
OB_13	6.74	32 kbp	7 kbp	1266	5928	34.40%	82
OB_14	6.81	436 kbp	121 kbp	365	6165	44.90%	17
OB_15	2.25	20 kbp	4 kbp	800	2345	36.10%	13

941

942

943

944

945 **Supplementary table S2:** Distribution of potential genes in involved in acidification. SPI refers
946 to Sec type signal peptides and SPII is used for lipoprotein signal peptides according to SignalP
947 (97).

MAG	P-type ATPase	Lactate dehydrogenase	Carbonic anhydrase
BB_1	1	1	2
BB_2	8	0	2 (1x SPI)
BB_3	13	1	2 (1x SPI)
BB_4	12	0	5 (1x SPI)
BB_5	2	1	2
BB_6	2	2	2
BB_7	2	0	1
BB_8	3	0	3 (1x SPI, 1x SPII)
BB_9	1	1	0
BB_10	2	0	3 (1x SPII)
BB_11	2	0	1 (1x SPII)
BB_12	0	0	0
BB_13	8	0	2 (1x SPI)
BB_14	1	0	2 (1x SPI)
BB_15	4	0	1
BB_16	14	0	3 (1xSPII)
BB_17	1	1	1
BB_18	0	1	1
BB_19	2	0	2
BB_20	14	2	3 (1x SPI)
BB_21	2	0	1
BB_22	1	1	1
BB_23	3	0	1
BB_24	2	0	2
BB_25	1	0	1
BB_26	2	1	3 (2x SPI)
BB_27	0	0	1
BB_28	4	0	1
BB_29	1	1	1
BB_30	1	0	2 (1x SPI)
BB_31	7	0	2
BB_32	1	0	1
BB_33	2	3	1

BB_34	15	0	5 (1x SPI)
BB_35	1	1	2
BB_36	13	0	3 (1x SPI)
BB_37	3	1	2
BB_38	1	2	0
BB_39	0	0	1
BB_40	3	1	0
BB_41	2	0	3 (1x SPI)
BB_42	1	2	1
BB_43	1	0	1
BB_44	1	0	2
OB_1	3	1	3
OB_2	3	0	3
OB_3	1	1	0
OB_4	1	0	1
OB_5	1	0	0
OB_6	1	0	2
OB_7	1	0	2 (1x SPI)
OB_8	4	1	1
OB_9	2	3	1
OB_10	2	0	1
OB_11	4	0	1
OB_12	1	0	2
OB_13	0	1	0
OB_14	5	2	0
OB_15	2	3	1

955 **Supplementary table S3:** *Colwellia* genomes used in this study for comparison to MAG BB5.

Name	NCBI BioProject accession number	Isolation source	Number of M9 collagenases
Colwellia piezophila	PRJNA182419	Deep-sea sediment	2
Colwellia psychrerythraea	PRJNA258170	*Terua* mussel	11
Colwellia hornerae	PRJNA516280	Arctic sea ice	0
Colwellia demingiae	PRJNA516284	Arctic sea ice	1
Candidatus *Colwellia aromaticivorans*	PRJNA478776	Microcosm experiments with oil in seawater	0
Colwellia echini	PRJNA420580	Sea urchin	0
Colwellia beringensis	PRJNA378583	Marine sediment, Bering Sea	1
Colwellia agarivorans	PRJNA371543	Coastal sea water	0
Colwellia marinimaniae	PRJDB5767	Amphipod from Challenger Deep	4
Colwellia sediminilitoris	PRJNA381102	Tidal flat, South Sea, South Korea	0
Colwellia polaris	PRJNA380006	Arctic sea ice	0
Colwellia mytili	PRJNA381102	Mussel *Mytilus edulis*	2
Colwellia aestuarii	PRJNA371561	Tidal flat Korea	0
Colwellia chukchiensis	PRJNA380006	Arctic ocean	1

956

957

958

959

960

961

962

963

964

Supplementary figures

Supplementary figure S1: A) ROV image of bone incubation experiment in the Byfjorden at 68 m depth, shown is a cow tibia. B) Bones retrieved from the Byfjorden after nine months of incubation, bacterial mats and blackening at the epiphysis can be seen.

Supplementary figure S2: SSU rRNA gene profiling of bone surface biofilms and *Osedax* metagenomes. Figures have been adapted from phyloFlash (79). A) Heatmap of most prominent bacterial orders in the investigated metagenomes in respect to percental abundance. B) Barplot of present taxa in the both sample types.

Supplementary figure S3: Maximum-likelihood tree of all 94 obtained carbonic anhydrases and relevant reference sequences from Capasso *et al.*, 2015 (40).

Supplementary figure S4: Genomic context of all identified M9 collagenase in the investigated MAGs. M9 collagenases are encircled in red, all genes potentially involved in collagen/proline utilization pathways are encircled in green. The graphic was made with SnapGene software (from GSL Biotech; available at snapgene.com).

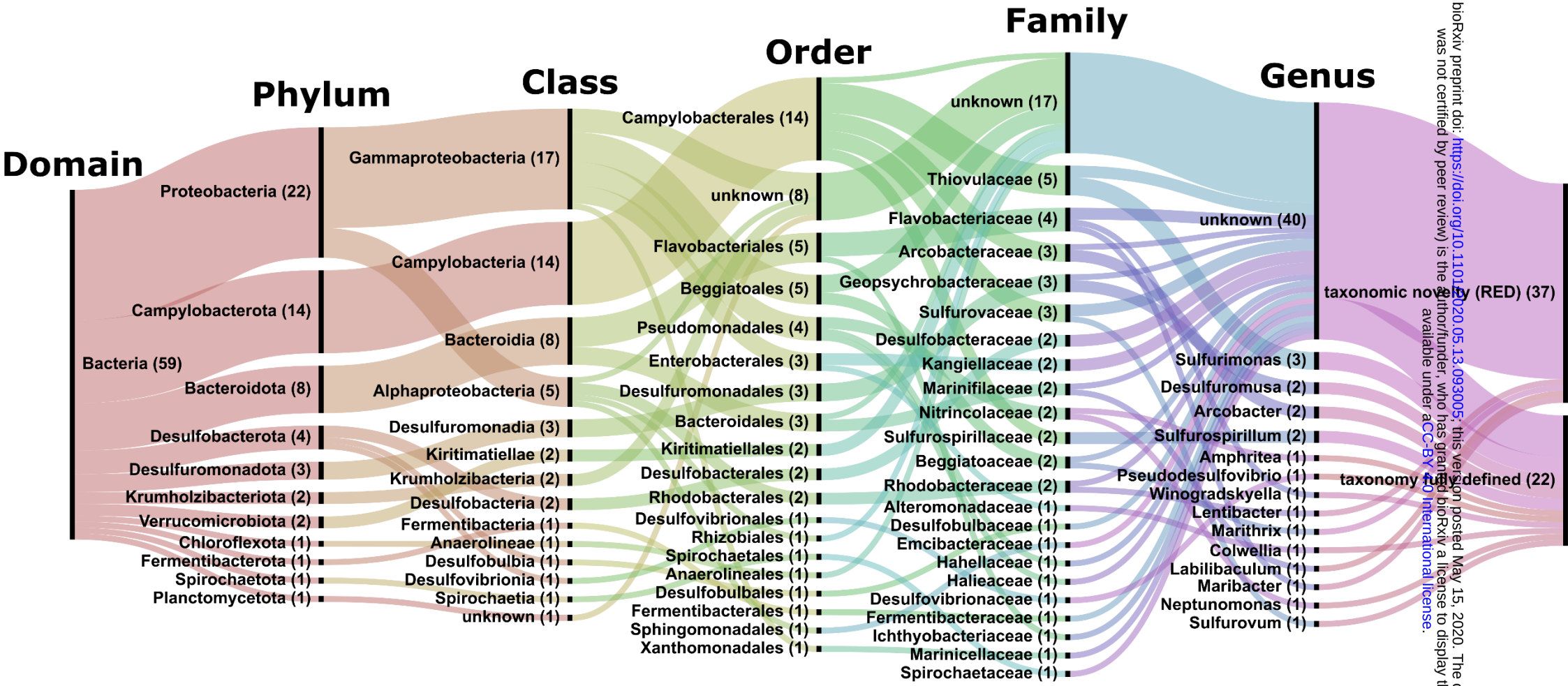

Figure 1: Alluvial diagram of the taxonomic affiliation of all 59 obtained high quality MAGs, spanning 11 phyla, 14 classes, 19 orders and at least 23 families. 37 out of 59 MAGs were identified as taxonomically novel as determined by their relative evolutionary divergence (RED) to their closest common ancestor. The taxonomic affiliation was inferred with GTDBTk (36) and visualized with RAWGraphs (86).

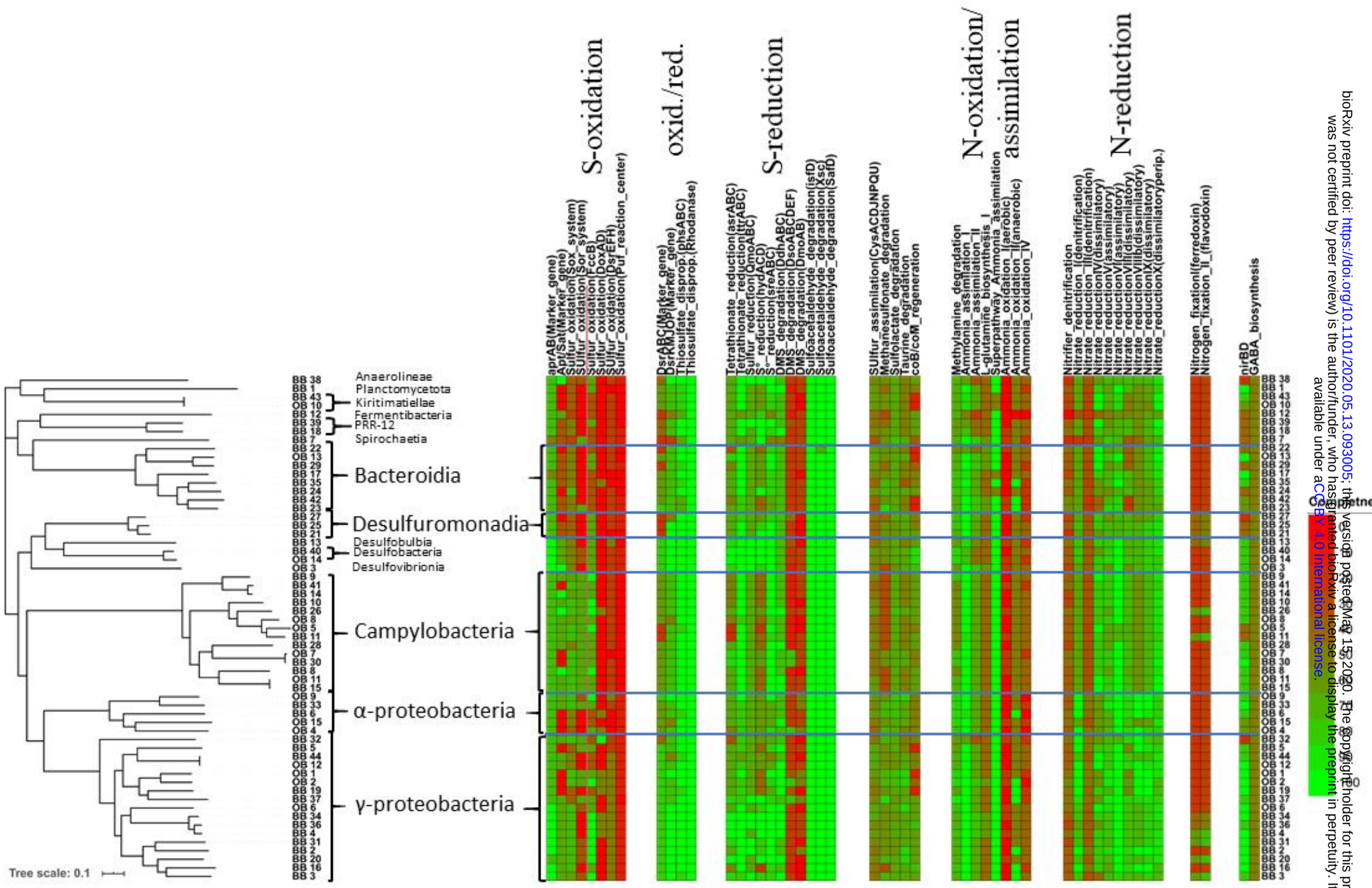

Figure 2: Whole genome metabolic pathway comparison. Analysis was done with MEBS (37) and MAGs are phylogenetically grouped according to GTDBTk pipeline (36). The color gradients are explained next to the heatmaps. The heatmap shows the presence of marker genes or completeness of different metabolic systems within the MAGs.

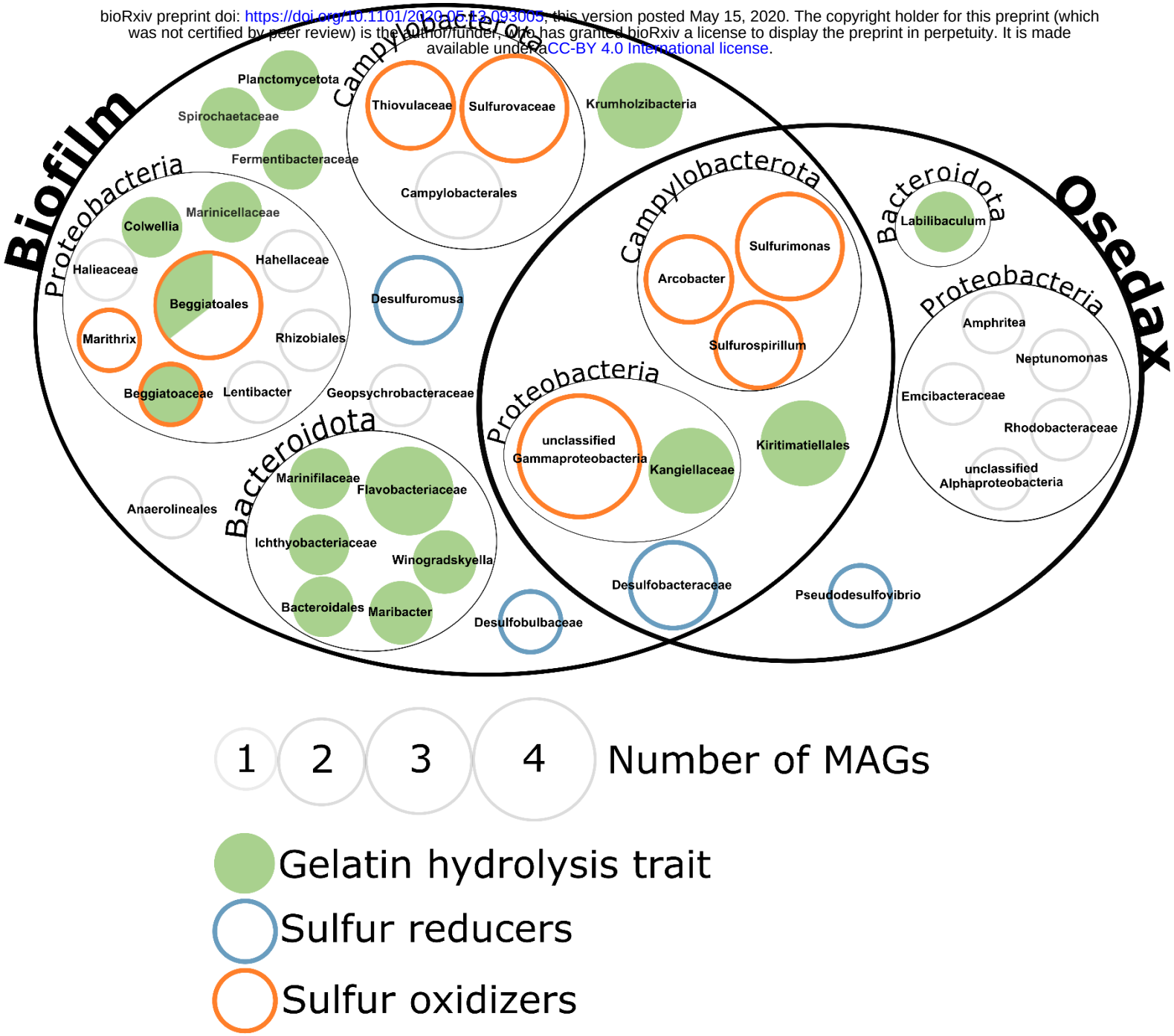

Figure 3: Taxonomic relationship, gelatin hydrolysis analysis, SRB and SOB within the surface communities (Biofilm) and *Osedax* metagenomes. MAGs are displayed with the deepest taxonomic classification obtained. Bacterial clades predicted to encode the gelatin hydrolysis trait are depicted in green according to analysis with Traitar (39), SRB are encircled in blue and SOB in orange.

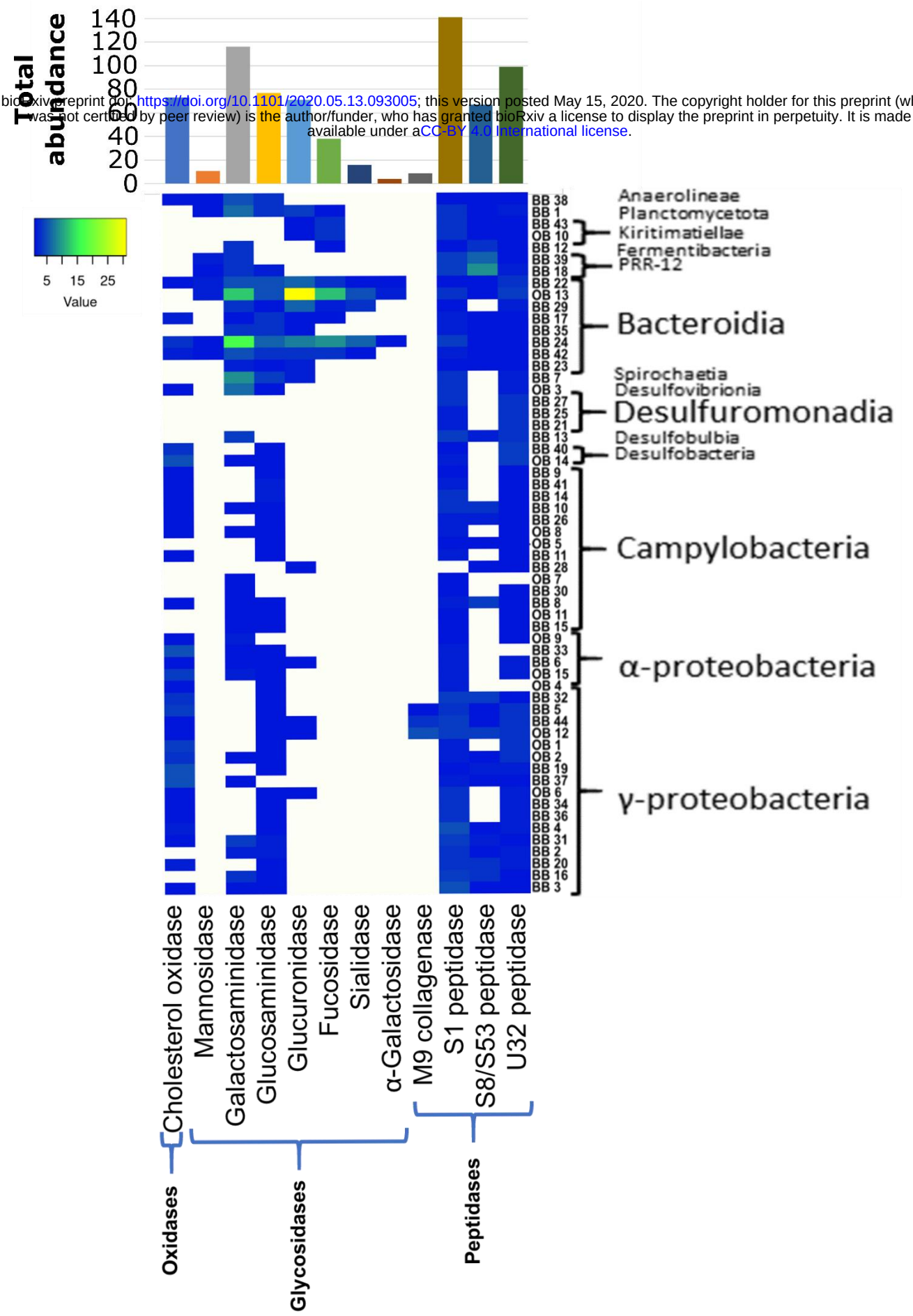

Figure 4: Presence of putative bone degrading enzymes in extracted MAGs. A) Abundance heatmap of the 12 investigated enzyme classes in the 59 high quality MAGs. The MAGs are arranged according to taxonomic affiliation. The absolute abundances of each enzyme class are depicted in the diagram on top of the heatmap. C) Percental distribution of all 722 identified enzymes according to their enzyme class.

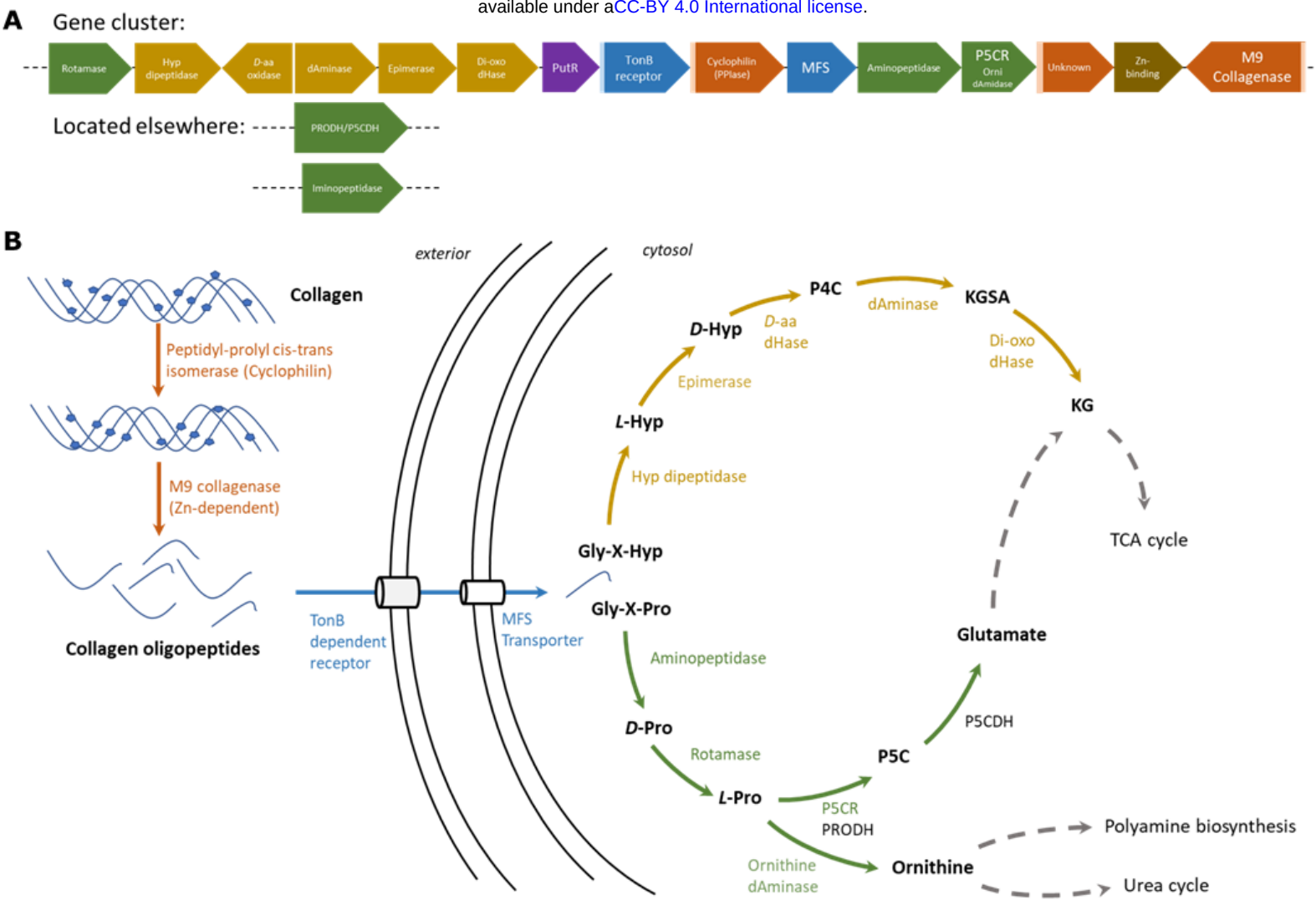

Figure 5: Collagen utilization in MAG BB5. A) Gene cluster in BB5, comprising 15 genes for collagen utilization, each color-coded respective to its functional group: orange for collagen hydrolysis, blue for uptake and transport, green for proline (Pro) utilization, ocher for hydroxyproline (Hyp) utilization and brown for unknown function. A light box is indicative of a predicted signal-peptide for secretion. B) Metabolic prediction model for functional collagen utilization in *Colwellia* BB5. Arrows and genes are color coded in the same functional groups as in A. Gray dotted arrows indicate a connection to a major metabolic pathway. Intermediate abbreviations: P4C (1-pyrroline 4-hydroxy-2-carboxylate), KGSA (alpha-ketoglutarate semialdehyde), KG (alpha-ketoglutarate), P5C (1-pyrroline-5-carboxylate). Enzyme abbreviations: D-aa dHase (D-hydroxyproline dehydrogenase), dAminase (pyrroline-4-hydroxy-2-carboxylate deaminase), di-oxo dHase (KGSA dehydrogenase), P5CR/ornithine dAminase (bifunctional 1-pyrroline-5-carboxylate reductase/ornithine cyclodeaminase), PRODH (proline dehydrogenase), P5CDH (pyrroline-5-carboxylate dehydrogenase).

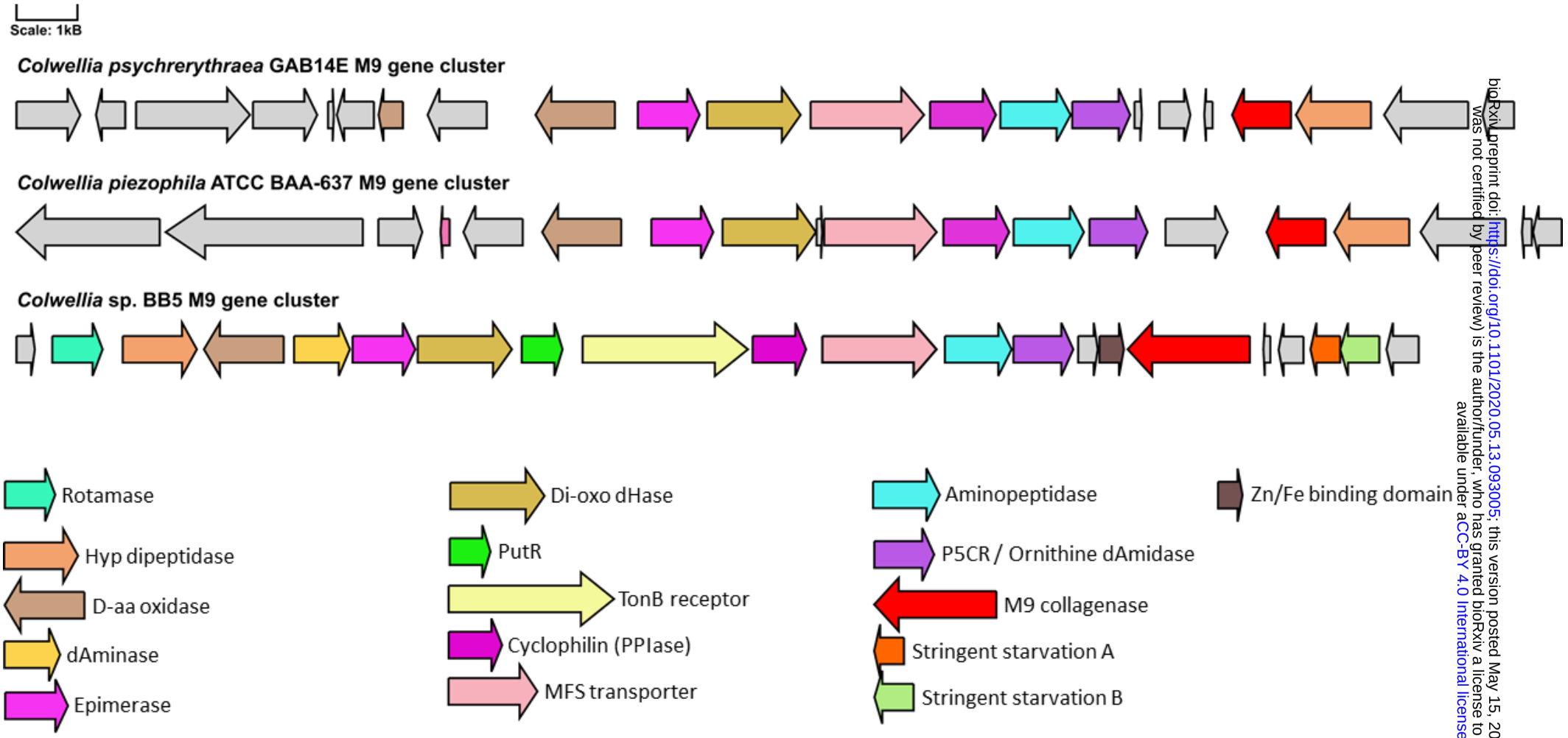

Figure 6: Conservation between M9 collagen degradation gene clusters in *Colwellia psychrerythraea* GAB14E, *Colwellia piezophila* ATCC BAA-637 and the MAG *Colwellia* BB5 drawn at scale. dHase, dehydrogenase; PPIase, peptidyl-prolyl cis trans isomerase; Hyp, D-aa, dAminase etc. Color coding and gene names are indicated.

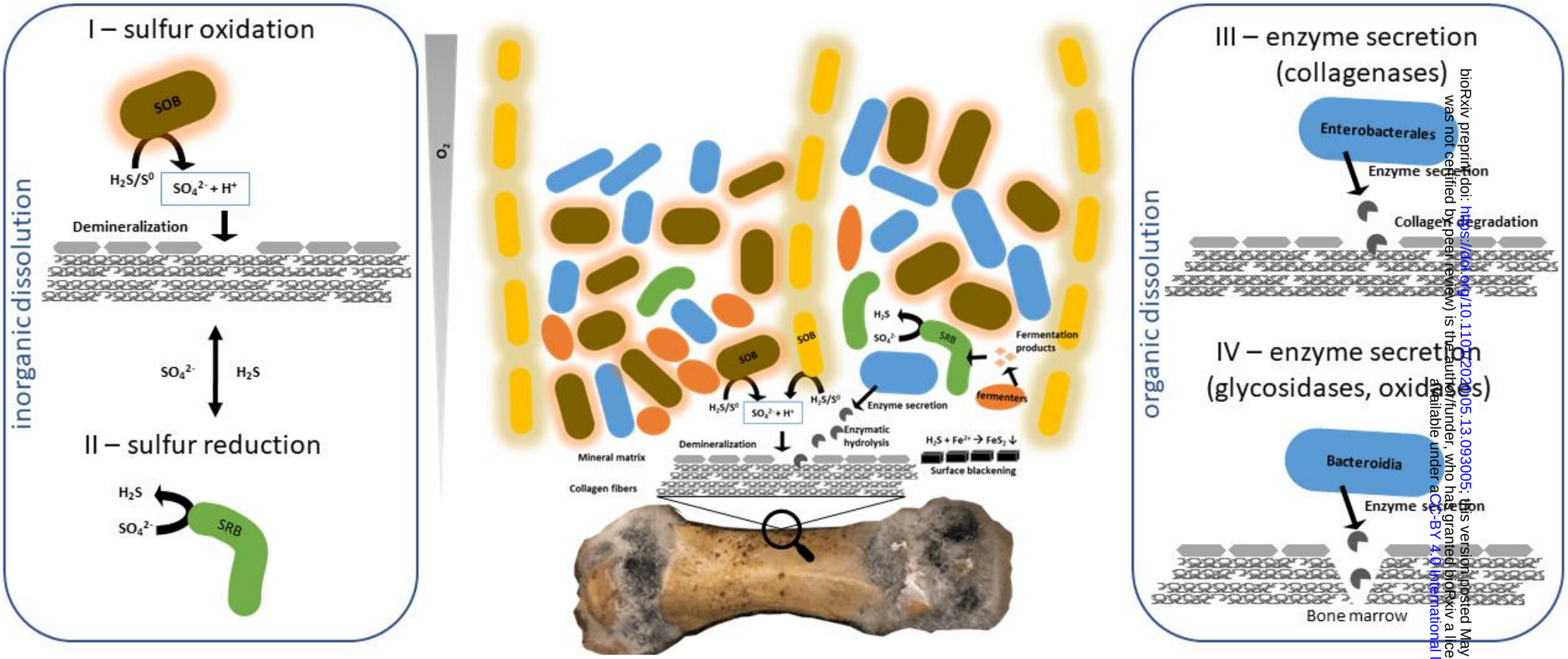

Figure 7: Hypothesis of the interplay in the marine bone microbiome and degradome. (I) Sulfur-oxidizing bacteria (SOB, shown with a halo) convert elemental sulfur and H_2S into sulfate and protons that lead to an acidification and therefore bone demineralization. (II) Sulfate reducing (SRB, green) and sulfur disproportioning bacteria produce H_2S from sulfate. (III) Enterobacterales and other especially γ-proteobatceria secret collagenases to degrade collagen. (IV) Bacteroidia and other bacteria secret gylcosidases and other enzymes to hydrolyze the organic bone components (glycosides, esters, lipids). This exemplifies a bone demineralization loop that fuels itself as long as sulfur is available and degrades the organic bone components in the process.